UPWIND MIXED ELEMENT-VOLUME: COMBINATION WITH MESH ADAPTATION, MULTILEVEL ALGORITHMS, MOVING MESHES

Alain DERVIEUX, François COURTY,

INRIA, 2004 route des Lucioles, 06902 Sophia-Antipolis, France,

http://www-sop.inria.fr/tropics/,

Bruno KOOBUS,

University of Montpellier II, CC-051, F-34095 Montpellier and INRIA

OVERVIEW (1)

1. MIXED ELEMENT VOLUME
2. MESH ADAPTION
3. MULTILEVEL PRECONDITIONING

MIXED ELEMENT-VOLUME:

- upwind-element MUSCL scheme
- LED/TVD formulation with upwind element
- 6th derivative stabilisation
- Low-Mach preconditioned stabilisation
- Moving grids : three conservations

Back to the fluid numerics (0) : M.E.V.

The Roe Flux Difference Splitting is installed in a vertex, edge-based, Mixed Element-Volume formulation of first-order spatial accuracy:

$$W_{ij} \;=\; W_i \;\; ; \;\; W_{ji} \;=\; W_j$$

$$\Phi_{ij} \;=\; 0.5(\Phi(W_{ij} + \Phi(W_{ji}) \;+\; 0.5\;\gamma_v\;|A|(W_{ji} - (W_{ij})$$

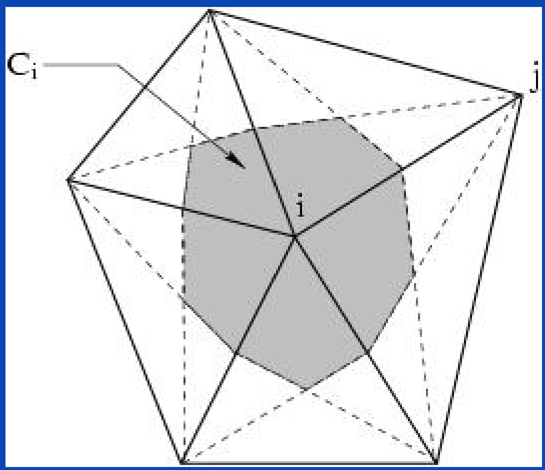

$$area(C_i)(W_i^{n+1} - W_i^n) \;+\; \Sigma\;\Phi_{ij} \;=\; 0$$

Back to the fluid numerics (1) : MUSCL

According to the MUSCL idea of van Leer, it is possible to transform a first-order spatially accurate Godunov scheme into a second-order one thanks to a linear reconstruction of dependant variables.

$$W_{ij} = W_i + \frac{1}{2}(\vec{\nabla}W)_{ij}.\vec{ij} \;\; ; \;\; W_{ji} = W_j - \frac{1}{2}(\vec{\nabla}W)_{ji}.\vec{ij}$$

$$\Phi_{ij} = 0.5(\Phi(W_{ij} + \Phi(W_{ji}) + 0.5\ \gamma_v\ |A|(W_{ji} - (W_{ij})$$

Our option is to use different edge-based reconstructions using the so-called called **upwind elements** of each edge.

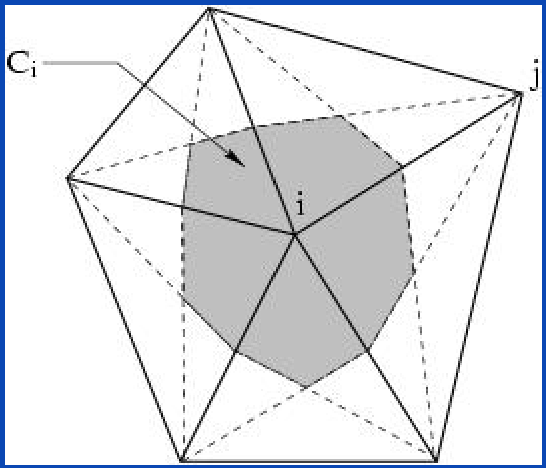

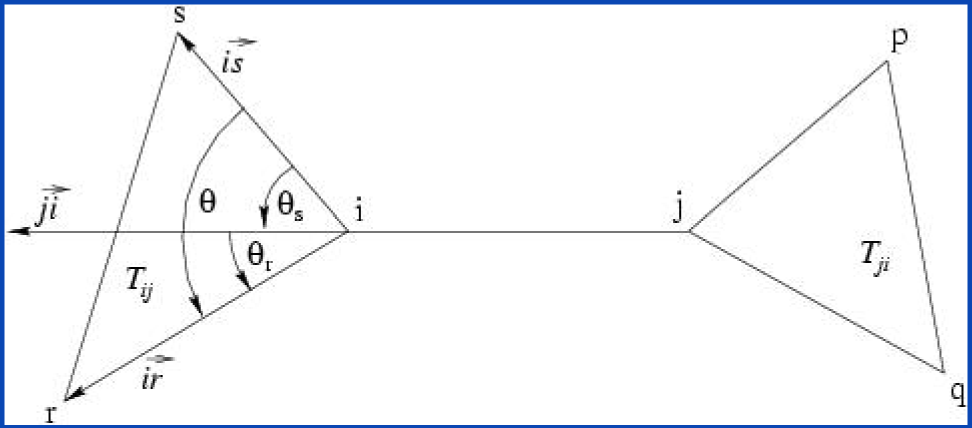

Back to the fluid numerics (2) : TVD/LED

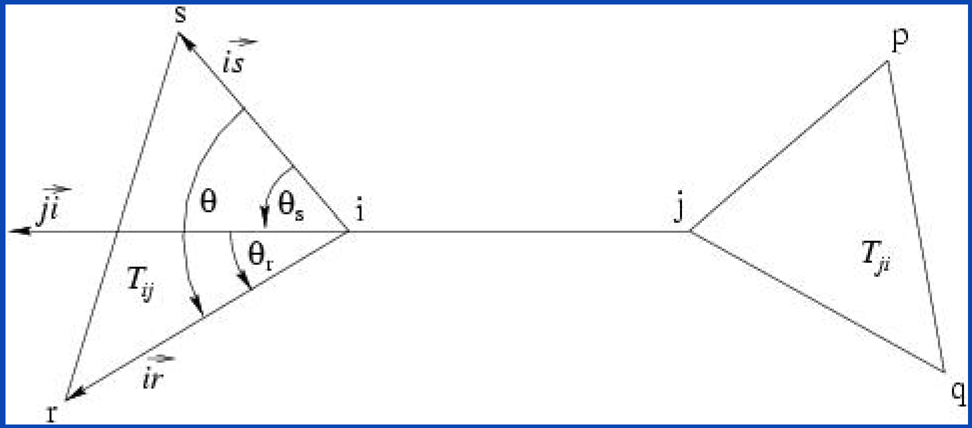

$$(\vec{\nabla}W)_{ij}.\vec{ij} = L(\Delta^{-}W_{ij}\,,\Delta^{0}W_{ij}\,,\nabla_{ij}W.\vec{ij})$$
$$(\vec{\nabla}W)_{ji}.\vec{ji} = L(\Delta^{-}W_{ji}\,,\Delta^{0}W_{ji}\,,\nabla_{ji}W.\vec{ji}). \qquad (1)$$

Second-order accurate density-positive scheme, satisfying the Maximum Principle for convected species
(Cournede-Debiez-Dervieux, INRIA report 3465,1998)

Back to the fluid numerics (3) : V6

The fourth-order derivative viscosity involved in the -unlimited- MUSCL scheme is still too viscous for many applications.

Much better accuracy is obtained by tuning its coefficient and still even better by using instead a sixth order derivative numerical viscosity.

This is realised in the MUSCL context by replacing a “linear” interpolation a cell boundary by a smarter interpolation:

$$W_{ij} \;=\; W_i \;+\; (\vec{\nabla} W)_{ij}^{\mathbf{V6}} . \vec{ij} \qquad (2)$$

Back to the fluid numerics (3) : V6 (end'd)

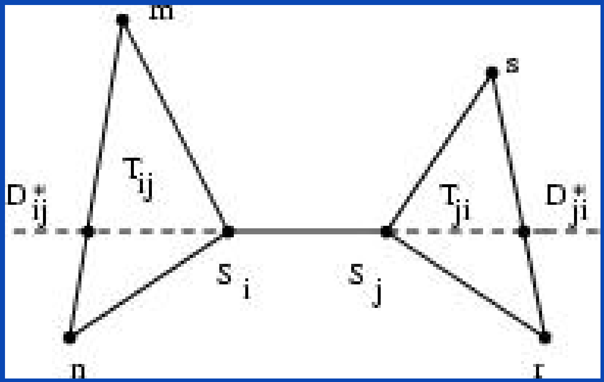

$$(\vec{\nabla}W)^{\mathbf{V6}}_{ij}.\vec{ij} \;=\; (1-\beta)\,(\vec{\nabla}W)^{C}_{ij}.\vec{ij} \;+\; \beta\,(\vec{\nabla}W)^{D}_{ij}.\vec{ij}$$
$$+\,\xi^a\,(\,(\vec{\nabla}W)_{T_{ij}} - 2(W_j - W_i) + (\vec{\nabla}W)_{T_{ji}})$$
$$+\,\xi^b\,(\,(\vec{\nabla}W)^{D^*}_{ij}.\vec{ij} \;-\; 2\,(\vec{\nabla}W)_i.\vec{ij} \;+\; (\vec{\nabla}W)_j.\vec{ij}\,) \qquad (3)$$

$(\vec{\nabla}W)^{D^*}_{ij}$: linear interpolation of **nodal gradients** in nodes m and n.
- Accurate enough for **acoustics**(Abalakin-Dervieux-Kozubskaya)

Back to the fluid numerics (3) : V6 ; an example

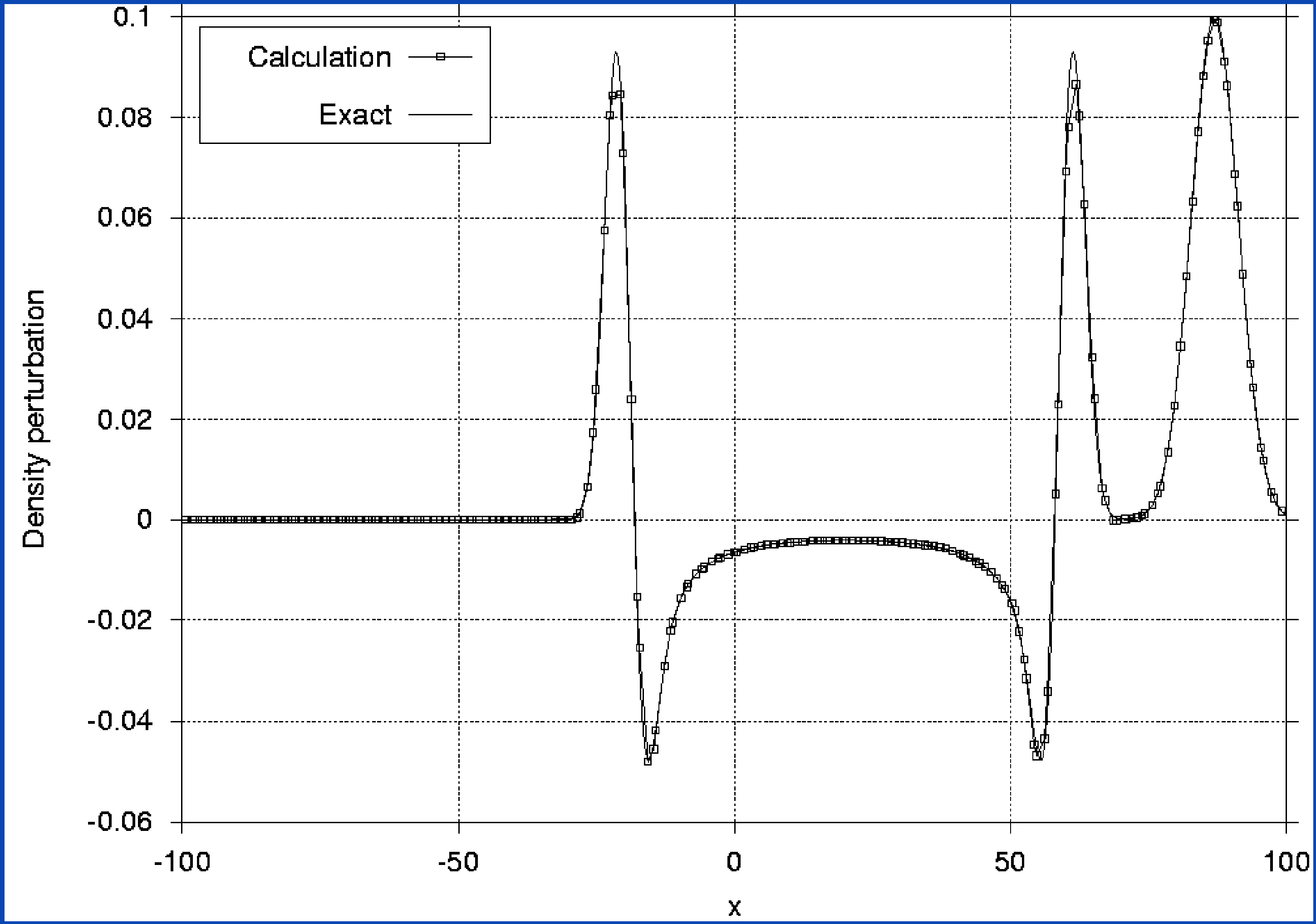

Back to the fluid numerics (4) : Low Mach

Godunov methods suffer larger truncation errors for smaller Mach number.

The Turkel preconditioner is then introduced in order to allow Mach-independant approximation errors.

$$\Phi(W_j,W_k,\vec{\eta}_{jk}) \;=\; 0.5(\mathcal{F}_j+\mathcal{F}_k).\vec{\eta}_{jk} + 0.5P(M_*)^{-1}|P(M_*)\mathcal{A}|(W_j-W_k).$$

Example from Schall-Viozat-Koobus-Dervieux, J. Heat and Mass Transfer, 2003

Low Mach ; Lid driven cavity, Re=1000

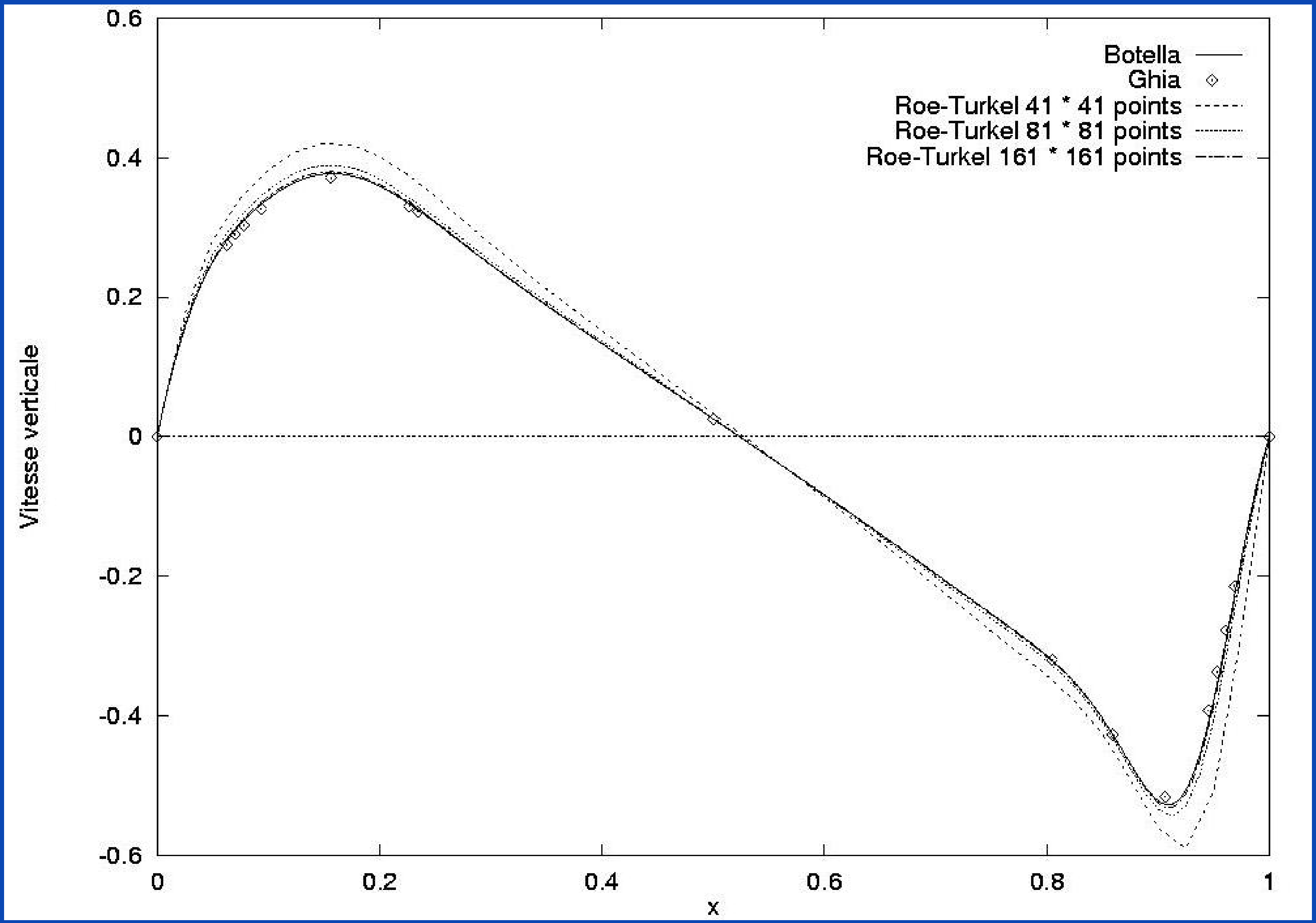

THE THREE CONSERVATIONS

- Conservation of extensive quantities.
- Geometric Conservation law.
- Energy budget.

Conservation of quantities

Local conservation of mass, moments energy is directly enforced in the gas field by ALE finite volumes .

It is an important consistency condition (Lax-Wendroff theorem).

It is a crucial condition for practical accuracy on non uniform meshes.

Geometric Conservation law

"A ALE-GCL scheme computes exactly a uniform flow field"

$$
\begin{aligned}
|\Omega_i^{n+1}|U_i^{n+1} &= |\Omega_i^n|U_i^n - \\
&\Delta t \sum_{j\in V(i)} |\partial\bar{\Omega}_{ij}|\ \Phi\left(U_i^{n+1}, U_j^{n+1}, \bar{\nu}_{ij}, \frac{x_{ij}^{n+1}-x_{ij}^n}{\Delta t}\right) \\
\bar{\nu}_{ij} &= 0.5\ \left(\nu_{ij}(x(t_1+\alpha_1(t_2-t_1))) + \nu_{ij}(x(t_1+\alpha_2(t_2-t_1)))\right) \\
\Rightarrow |\Omega_i^{n+1}| - |\Omega_i^n| &= \int_{\partial\Omega_h(t)} \dot{x}_i\, n_i\, d\Gamma
\end{aligned}
$$

- sufficient condition for 1st-order accuracy (Guillard-Farhat).
- Maximum Principle (Farhat-Geuzaine-Grandmont).
- Practical stability and accuracy improvements.

Energy budget

Structure models are generally made of a finite element variational principle and satisfy a discrete energy conservation.

- **Work transfer** between **non-conforming** fluid and structure:

- spatially non-conforming: energy conserving integrations of forces and motion (Farhat-Lesoinne-Le Tallec).

- time staggering: energy conservation enforced up to 4th order (Piperno-Farhat).

Energy budget of fluid (1)

The energy equation **must** satisfy the Geometric Conservation Law and this is obtained by an adhoc time integration:

$$|\Omega_i^{n+1}|\ E_i^{n+1} \quad =$$

$$|\Omega_i^n| E_i^n - \Delta t \sum_{j \in V(i)} |\partial \bar{\Omega}_{ij}|\ \Phi^E \left(U_i^{n+1}, U_j^{n+1}, \bar{\nu}_{ij}, \frac{x_{ij}^{n+1} - x_{ij}^n}{\Delta t} \right)$$

$\bar{\nu}_{ij}$ specified by GCL.

Energy budget of fluid (2)

Work transfers:

$$\Delta \mathbf{M}\Big|_{t_1}^{t_2} \cdot \left(\mathbf{x}_{ij}^{n+1} - \mathbf{x}_{ij}^{n}\right) \;=$$

$$\Delta t \sum_{i \in \partial\Omega_h} |\partial\bar{\Omega}_{h,i}| \; \Phi_{\partial\Omega}^{M} \left(W_i^{n+1}, \bar{\nu}_{ij}, \frac{x_{ij}^{n+1} - x_{ij}^{n}}{\Delta t} \right) \; \cdot \left(\mathbf{x}_{ij}^{n+1} - \mathbf{x}_{ij}^{n}\right)$$

$$\Delta Work\Big|_{t_1}^{t_2} \;=\; \Delta t \sum_{i \in \partial\Omega_h} |\partial\bar{\Omega}_{h,i}| \; p_i \; \bar{\nu}_i \; . \; \dot{x}_i$$

Energy budget of fluid (3)

Total energy variation:

$$\Delta E \Big|_{t_1}^{t_2} = \Delta t \sum_{i \in \partial\Omega_h} |\partial\bar{\Omega}_{h,i}| \; \Phi^E_{\partial\Omega} \left(W_i^{n+1}, \bar{\nu}_{ij}, \frac{x_{ij}^{n+1} - x_{ij}^{n}}{\Delta t} \right)$$

$$\Delta E \Big|_{t_1}^{t_2} = \Delta t \sum_{i \in \partial\Omega_h} |\partial\bar{\Omega}_{h,i}| \left(\int_{\partial\Omega_{h,i}} p_i \, u_i \, . \, \bar{\nu}_i \, d\Gamma \right)$$

Energy budget of fluid (4)

$$\Delta E\Big|_{t_1}^{t_2} = \Delta t \sum_{i \in \partial\Omega_h} |\partial\bar{\Omega}_{h,i}|\; p_i\; \bar{\nu}_i \;.\; \dot{x}_i$$

Lemma: *By replacing the energy flux by a product of boundary pressure times the GCL integration of mesh motion, we can derive a scheme that is conservative, satisfies GCL and have an exact energy budget (work of pressure = loss of total energy).*

The band of the three conservations: synthesis

The recent works have proved that is is possible to build a scheme that satisfies the following properties:

- Conservation,

- Geometric Conservation Law, and maximum principle (applying to K, ϵ, species,..),

- Accurate energy complete budget.

COMPLEXITY OF COMPUTATIONAL MECHANICS (1)

Complexity in Computational Continuum Mechanics:

How many arithmetic operations for obtaining an approximation of the PDE solution with a given accuracy?

- approximation: what accuracy when N unknown are used?

- algorithmics: how many operations for finding these N unknowns?

COMPLEXITY OF COMPUTATIONAL MECHANICS (1)

I. Continuous models for adaptation.

II. Multilevel preconditioning

II. CONTINUOUS MODELS FOR ADAPTATION

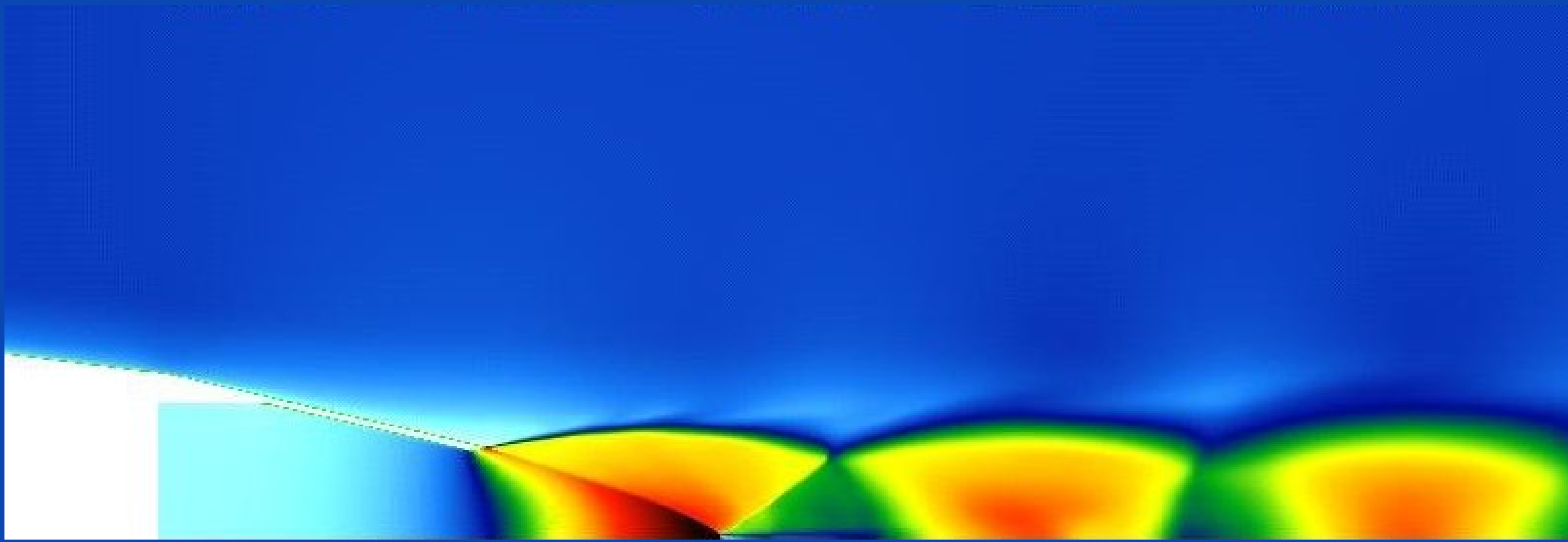

Afterbody flow ; supersonic ; turbulent.

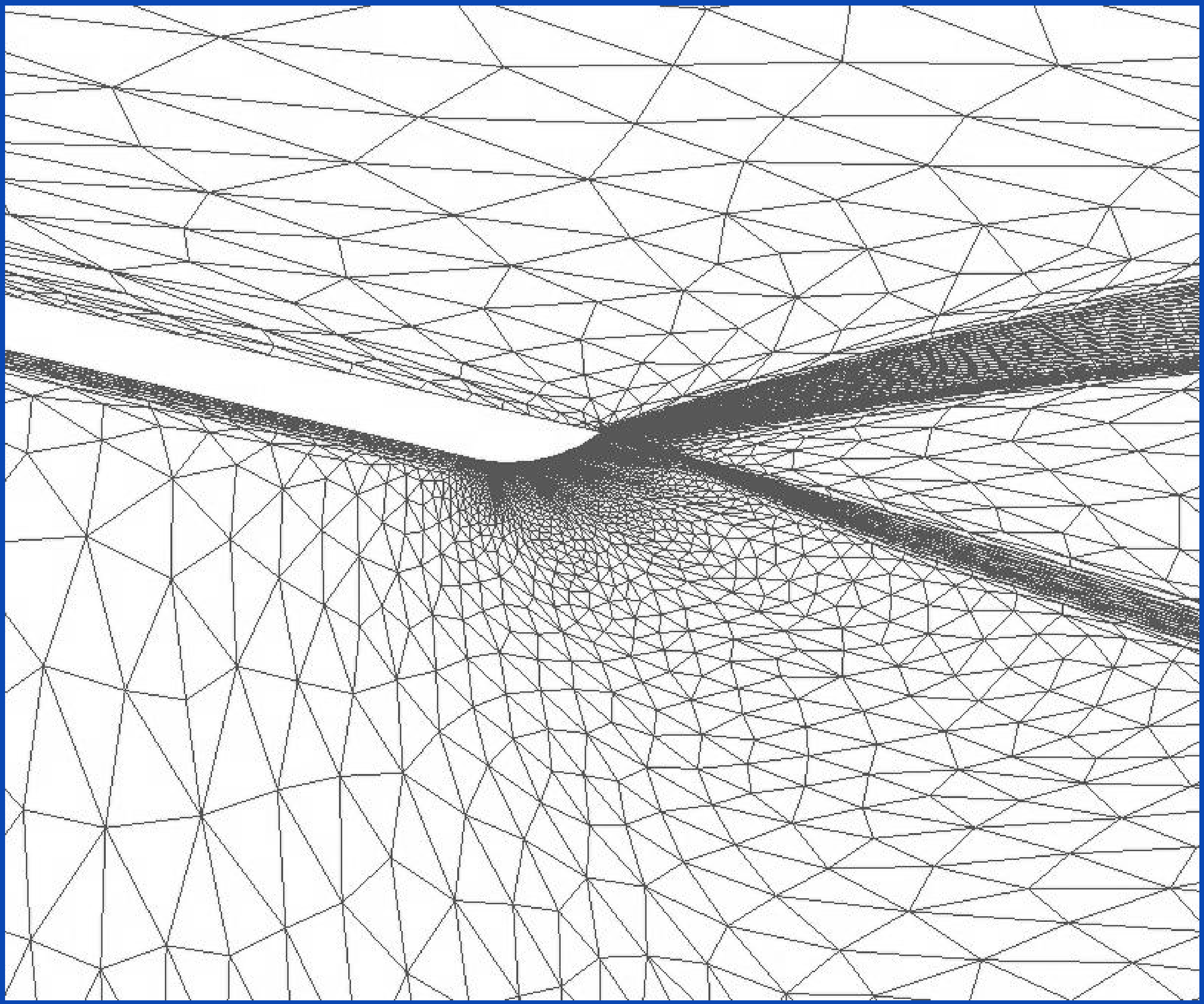

Convergence issue

Let us try to converge to the continuous limit by uniform refinement.

Test case conditions: NACA0012, Reynolds 73., Mach 1.2

Numerical scheme : vertex centered, upwind-MUSCL

- Should be second-order accurate:

$$\|u - u_h\|_{L^2} \leq Kh^2$$

Uniform refinement:

Uniform refinement : mesh 1, 800 vertices, mesh 2, 3114 vertices

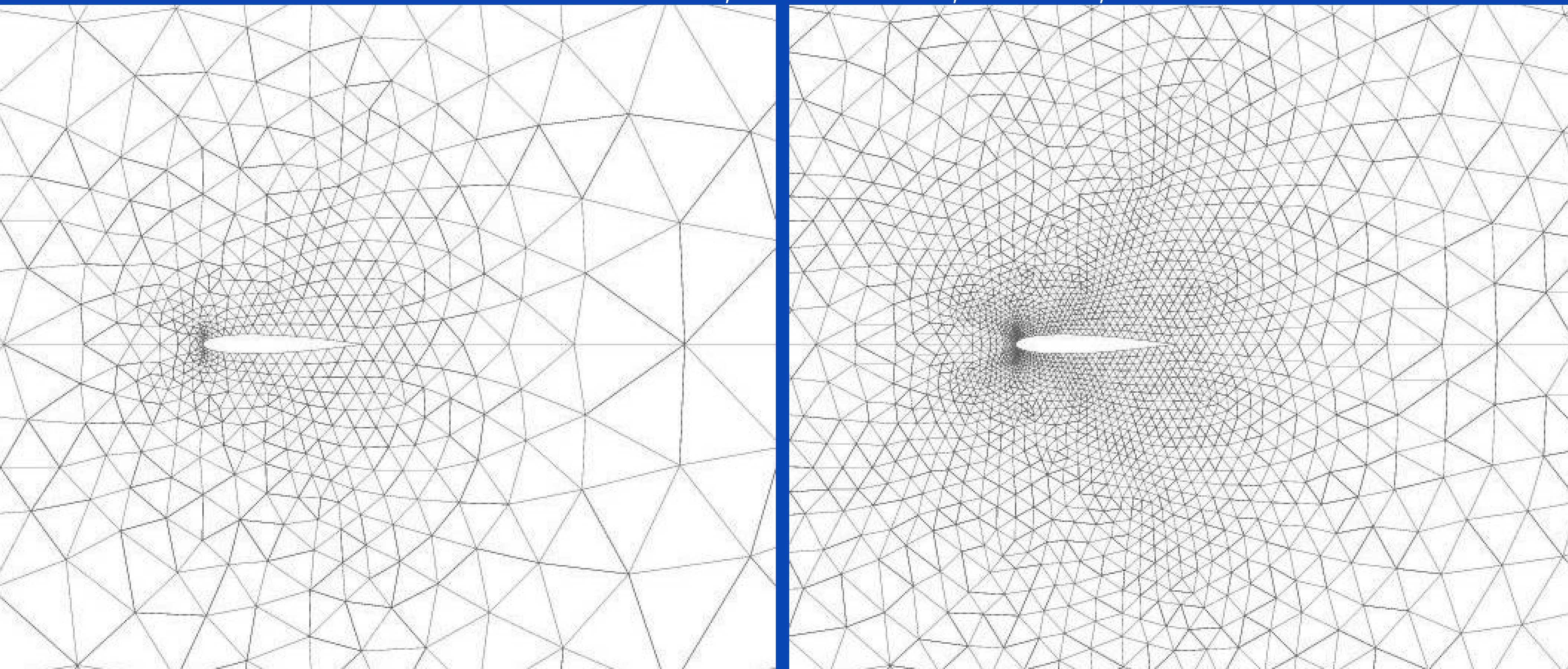

Uniform refinement : mesh 3, 12284 vertices, mesh 4, 48792 vertices

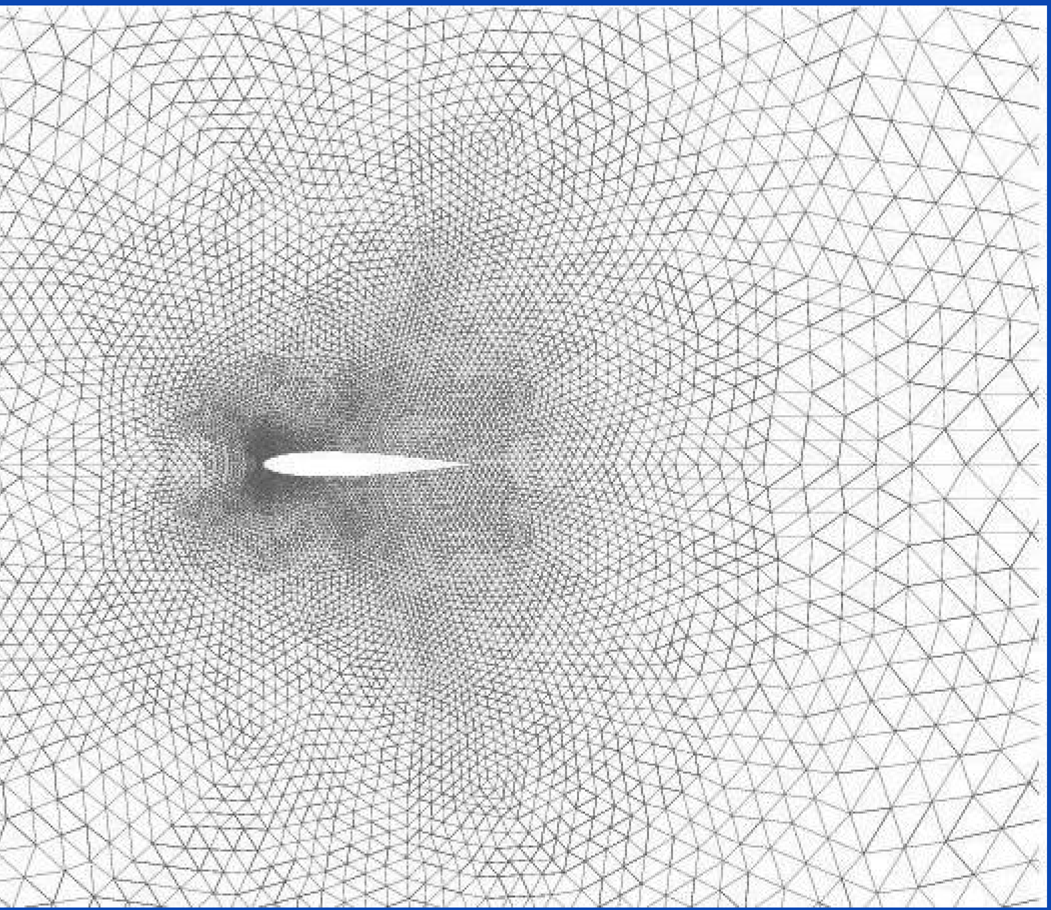

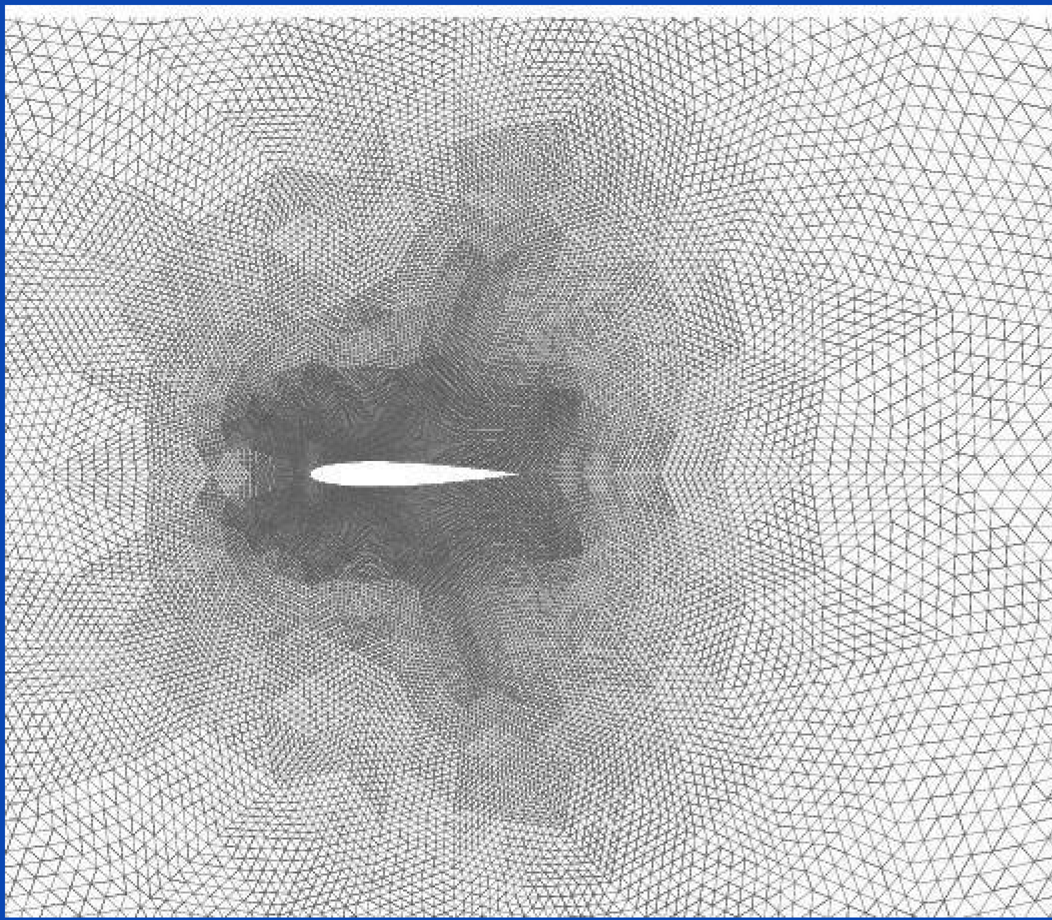

Convergence issue, concl'd

Let us measure the numerical order of convergence α :

$$\frac{\|U_1 - U_2\|_{L^2}}{\|U_2 - U_3\|_{L^2}} = \frac{1 - (1/2)^\alpha}{(1/2)^\alpha - (1/4)^\alpha} \quad ?$$

Meshes with 800, 3114, 12284 vertices: convergence order for the density field ρ : 0.94 ,

Meshes with 3114, 12284, 48792 vertices: convergence order for ρ : 1.14 .

The scheme is bad or the meshes are bad...

MESH ADAPTIVE INTERPOLATION : THE PROBLEM

- Let be u a *given* function (e.g. analytically defined).

- Find the mesh $\mathcal{M}_N$ with N vertices that interpolates with a continuous piecewise P_1 interpolent at best function f for the norm L^2 :

$$\mathcal{M}_N? \ \ such \ \ that \ \ \|u - \Pi_{\mathcal{M}_N} u\|_{L^2} = min \ .$$

- Compare:
. uniform refinement: $\Delta x = \frac{1}{N}$
. adaptative mesh series: $\mathcal{M}_N$, $N \to \infty$.

- Measure the order α of convergence:

$$\|u - \Pi_{\mathcal{M}_N} u\|_{L^2} \leq N^{-\frac{\alpha}{d}}$$

Best mesh: The “continuous metrics” approach, 1D

Instead of looking for a mesh of [0,1], we look for a *continuous local mesh size :*

m gives the size of Δx at point x, m^{-1} is the density of nodes, i.e. the number of nodes per length unit.

Let us work at a fixed number N of nodes.

Find $m : x \rightarrow m(x)$, with a given complexity:

$$C(m) = \int_0^1 m^{-1}(x)dx = N \ , \tag{4}$$

That minimizes the interpolation error.

Best mesh: The "continuous metrics" approach, 1D, smooth

In the case of P_1 interpolation, we modelize the interpolation error as :

$$\int_0^1 |e_{\mathcal{M}}(x)|^2 ds = \int_0^1 (m^2 |\frac{\partial^2 u}{\partial x^2}|)^2 ds. \quad (5)$$

Then (u smooth and never linear):

$$m_{opt}(x) = K \ N^{-2} (|u''(x)|)^{\frac{-2}{5}}. \quad (6)$$

High order adaptation for a discontinuity

u: bounded, piecewise smooth, with a few discontinuities.

Prototype : the Heavyside function $+$ a smooth function, on $[0,1]$.

Lemma: *For a uniform refinement, the order of accuracy in L^2 of the P1 interpolation is only 1/2. Conversely, there exist adaptative refinements for which the order of accuracy of P1 interpolation is 2.*

Idea of the proof : Divide the interval around discontinuity into eight intervals of same size and divide other intervals into two. Total mesh size is only increased by a factor $2 + 8/N$ and error is 4 times smaller.

N.B.: For a third-order P_2 interpolation, third-order accuracy is obtained by dividing the singular interval into 16.

The "continuous metrics" approach, 1D, non smooth

In the case of P_1 interpolation, we modelize the error as :

$$\int_0^1 |e_{\mathcal{M}}(x)|^\alpha ds = \int_0^1 (m^2|\delta^{-2}(u(x+\delta)-2u(x)+u(x-\delta))|)^\alpha ds.$$

where δ is smaller than m.

$\delta^{-2}(u(x+\delta)-2u(x)+u(x-\delta))$:

- is close to $\frac{\partial^2 u}{\partial x^2}$,

- or to δ^{-2},

- bounded in $L^{1/2}$ independantly of δ.

Continuous metrics adaption for a discontinuity

$$m_{opt}(x) = Cte.|(|\delta^{-2}(u(x+\delta) - 2u(x) + u(x-\delta))|(x))|^{\frac{-2}{5}}.$$

Further the resulting error in L^2 writes:

error $= \frac{2}{N^2} \left(\int |\delta^{-2}(u(x+\delta) - 2u(x) + u(x-\delta))|^{\frac{2}{5}} \right)^{\frac{5}{2}} < \frac{K}{N^2}$

which gives second-order accuracy.

Dicontinuity capturing: Numerical illustration:

Two examples : smooth arctangent, discontinuous Heavyside.

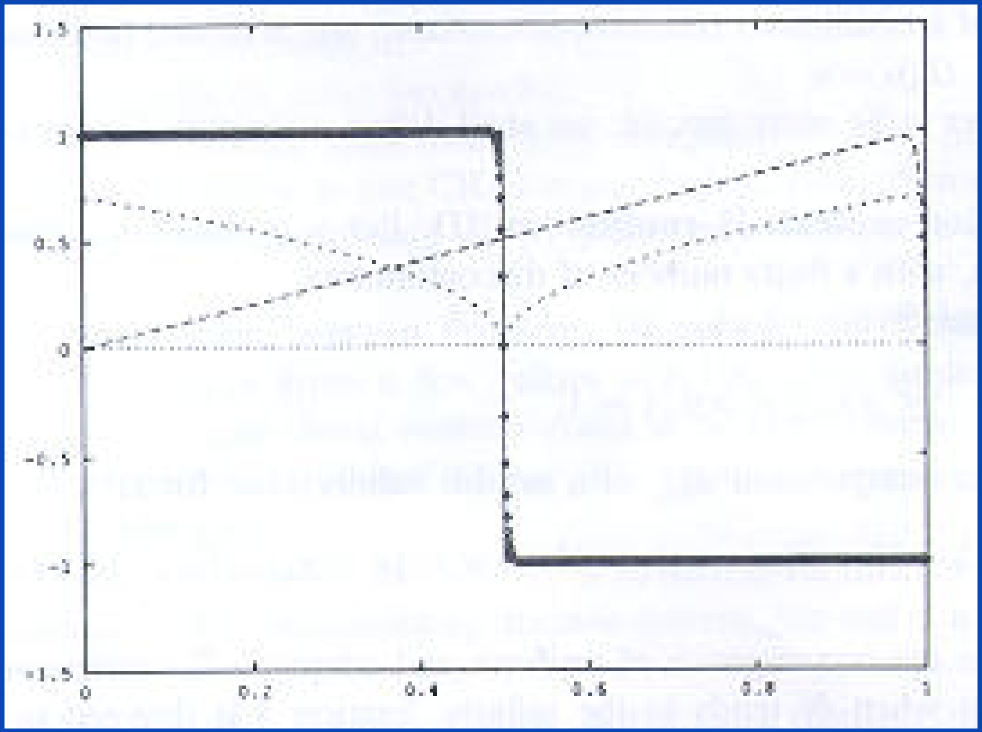

Adaptation on an interval :

Choose a number of nodes N.

Derive the optimal metrics m.

Define x from:

$$x_0 = 0, \qquad \int_{x_i}^{x_{i+1}} m^{-1} dx = 1 \ ,$$

N.B.: Can also be done by mesh deformation.

Convergence to the continuous: Heavyside

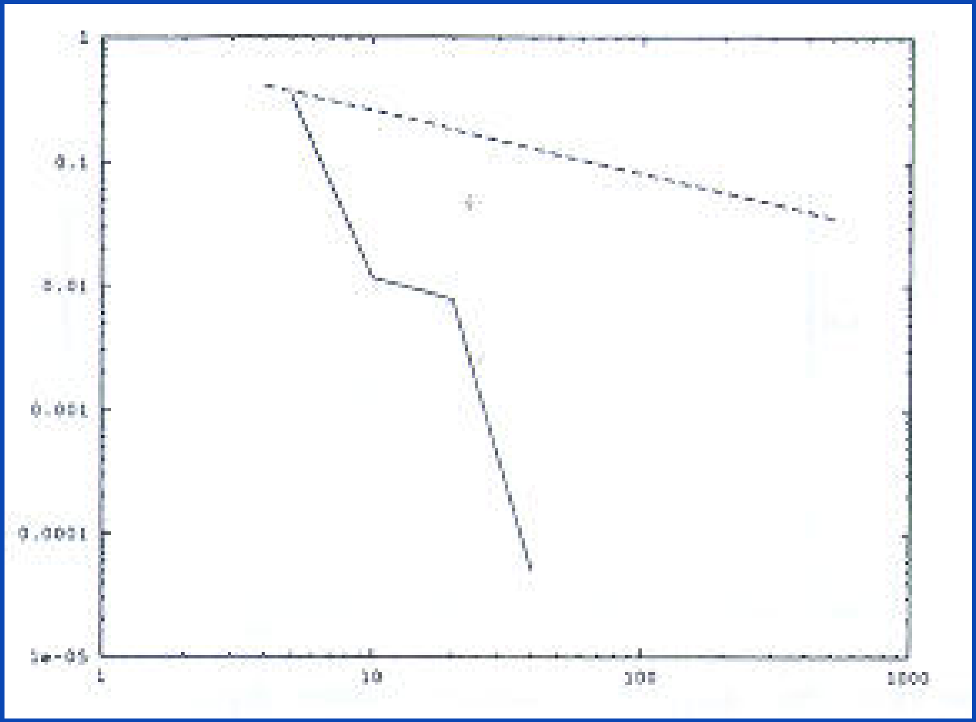

Convergence towards $y = -sign(x - \frac{1}{2})$

Abscissae : number of nodes; ordinates : interpolation error

Dashes : uniform refinement, line : adaptive refinement.

Convergence to the continuous: Arctangent

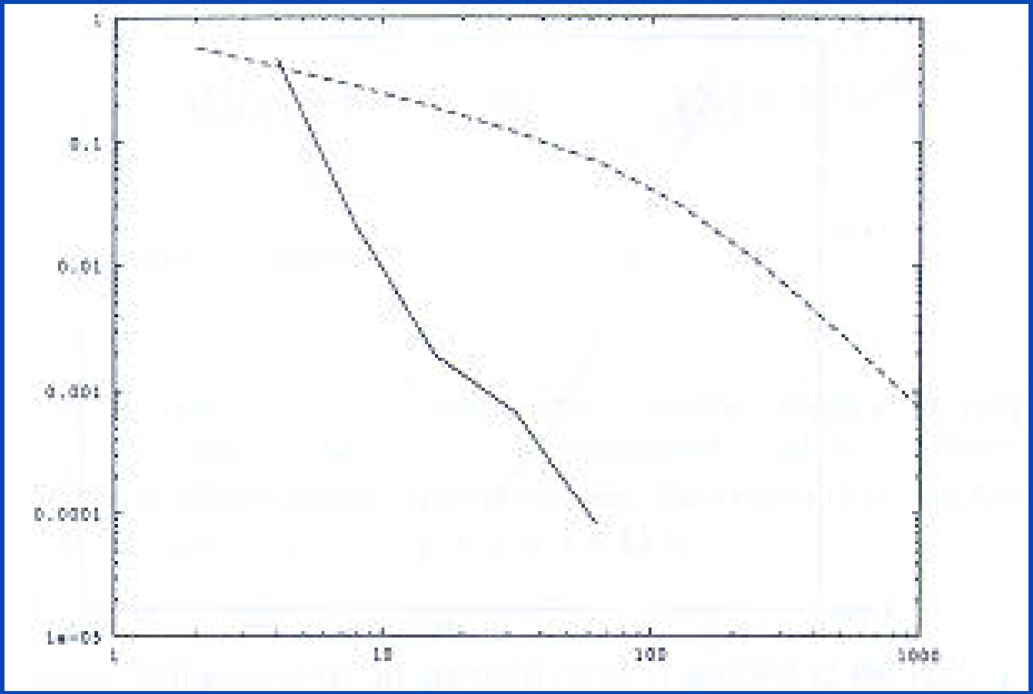

Uniform refinement: late capturing
Adaptative refinement : early capturing

Early capturing/late capturing

Uniform refinement needs N_S nodes, where N_s is the inverse of the size of the smallest detail (1D).

A good adaptative refinement needs N_d nodes, where N_d is (1D) the number of details (for example: the function is monotone on N_d intervals).

$$N_d \quad << \quad N_S.$$

The "continuous metrics" approach, 2D

In short we look for metrics

$$\mathcal{M}_{x,y} = \mathcal{R}_{\mathcal{M}}^{-1} \begin{pmatrix} (m_\xi)^{-2} & 0 \\ 0 & (m_\eta)^{-2} \end{pmatrix} \mathcal{R}_{\mathcal{M}} \tag{7}$$

When a mesh satisfies the metrics, this operator tranforms any edge in an edge with unit length.

This essentially specifies one mesh.

(George, Hecht,..., Fortin, Habashi,...)

First option : the metrics is aligned with the Hessian of u:

$$\mathcal{R}_{\mathcal{M}} \quad = \quad \mathcal{R}_u \ , \tag{8}$$

$\mathcal{R}_u$ diagonalises the Hessian $\mathcal{H}_u$ of u:

$$\mathcal{H}_u = \begin{pmatrix} \frac{\partial^2 u}{\partial x^2} & \frac{\partial^2 u}{\partial x.\partial y} \\ \frac{\partial^2 u}{\partial x.\partial y} & \frac{\partial^2 u}{\partial y^2} \end{pmatrix} = \mathcal{R}_u * \begin{pmatrix} \frac{\partial^2 u}{\partial \xi^2} & 0 \\ 0 & \frac{\partial^2 u}{\partial \eta^2} \end{pmatrix} * \mathcal{R}_u{}^{-1} \tag{9}$$

The "continuous metrics" approach, 2D, cont'd

$$\min_{\mathcal{M}} \int \left(|\frac{\partial^2 u}{\partial \xi^2}|.m_\xi^2 + |\frac{\partial^2 u}{\partial \eta^2}|.m_\eta^2 \right)^2 \; dxdy \qquad (10)$$

under the constraint $\int m_\xi{}^{-1} m_\eta{}^{-1} \; dxdy = N.$

according to a recent interpolation error estimate derived by George.
(Dervieux-George-Leservoisier INRIA Report, 2001).

The "continuous metrics" approach, 2D, cont'd

$$\mathcal{M}_{opt} = C^{-1}\ \mathcal{R}^{-1} \begin{pmatrix} |\frac{\partial^2 u}{\partial \eta^2}|^{-5/6} |\frac{\partial^2 u}{\partial \xi^2}|^{1/6} & 0 \\ 0 & |\frac{\partial^2 u}{\partial \xi^2}|^{-5/6} |\frac{\partial^2 u}{\partial \eta^2}|^{1/6} \end{pmatrix} \mathcal{R}\ .$$

with:

$$C_\alpha \ = \ \left(\int \left(|\frac{\partial^2 u}{\partial \xi^2}| . |\frac{\partial^2 u}{\partial \eta^2}| \right)^{\frac{\alpha}{2\alpha+2}} \ dxdy \right)^{-1} N\ .$$

Isotropic simplified optimum :

The above calculation can be done with a scalar metrics. It turns like the 1D case.

$$e_{\mathcal{M}}(x,y) \; = m^2(x,y)M(x,y)$$

where $M(x,y)$, is $Max(Sp(\mathcal{H}))$, the maximum absolute value of eigenvalues of the local Hessian of u. We obtain the optimum:

$$m_{opt}(x) = \left(\frac{(\int_\Omega M^{\frac{-2}{3}} ds)}{N} \right)^{\frac{1}{2}} \; M(x,y)^{\frac{-1}{3}}.$$

Numerical illustration : 1. Isotropic adaptive refinement

Test case : interpolate a couple of S-shaped arctangent functions
Sensor : scalar field equal to $Max(sp(\mathcal{H}))$.
Controlled Voronoi remeshing.George, Hecht, Saltel, Mohammadi,...

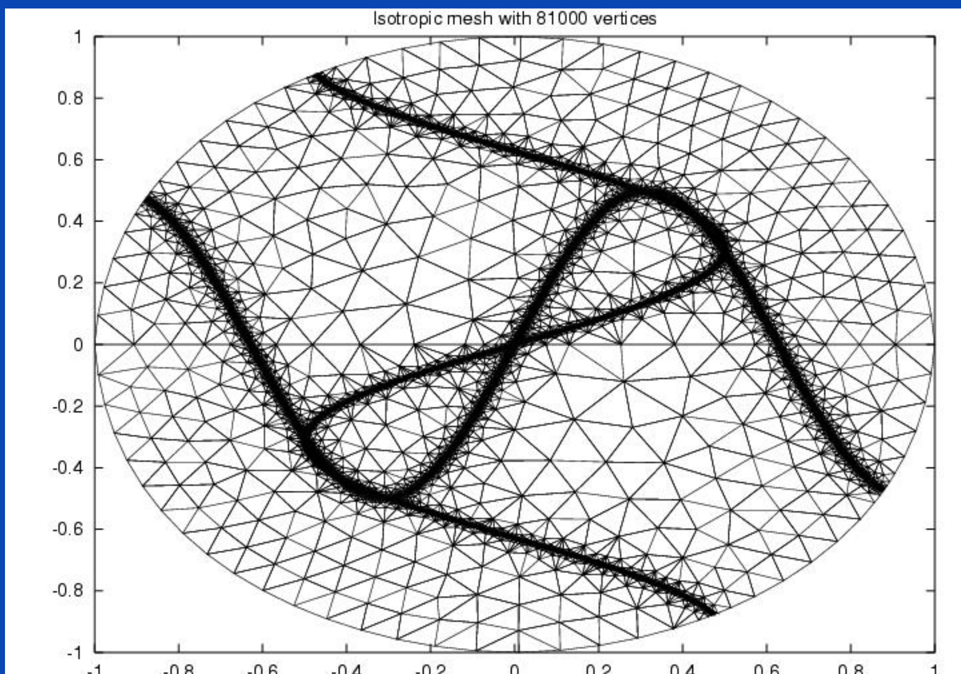

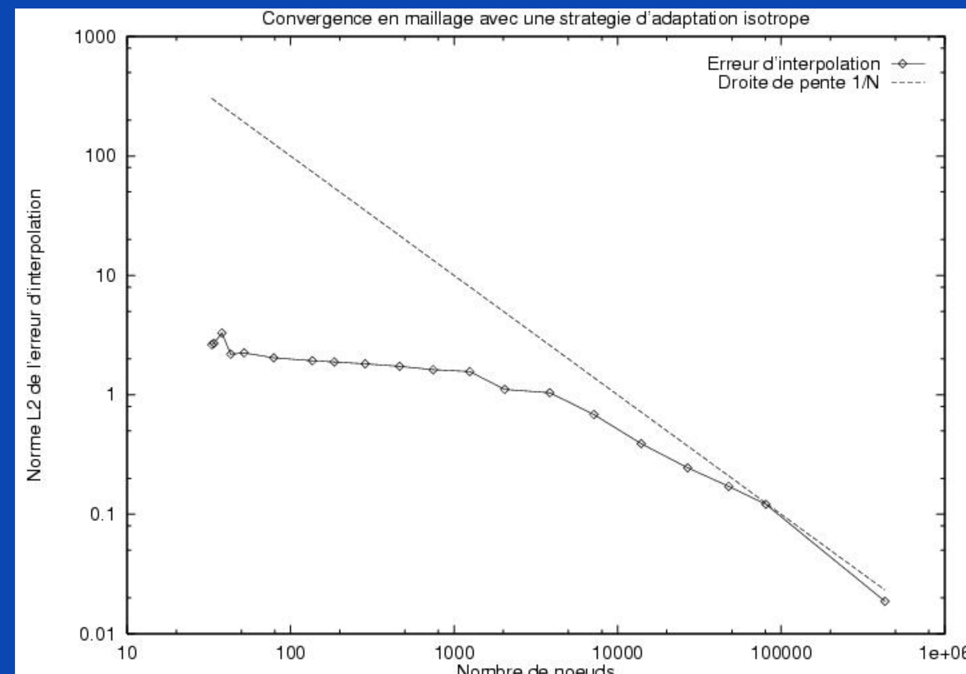

2. Anisotropic adaptive refinement

. Sensor : 2×2 metrics field derived from the Hessian
.Controlled Voronoi remeshing George, Hecht, Saltel, Mohammadi,..

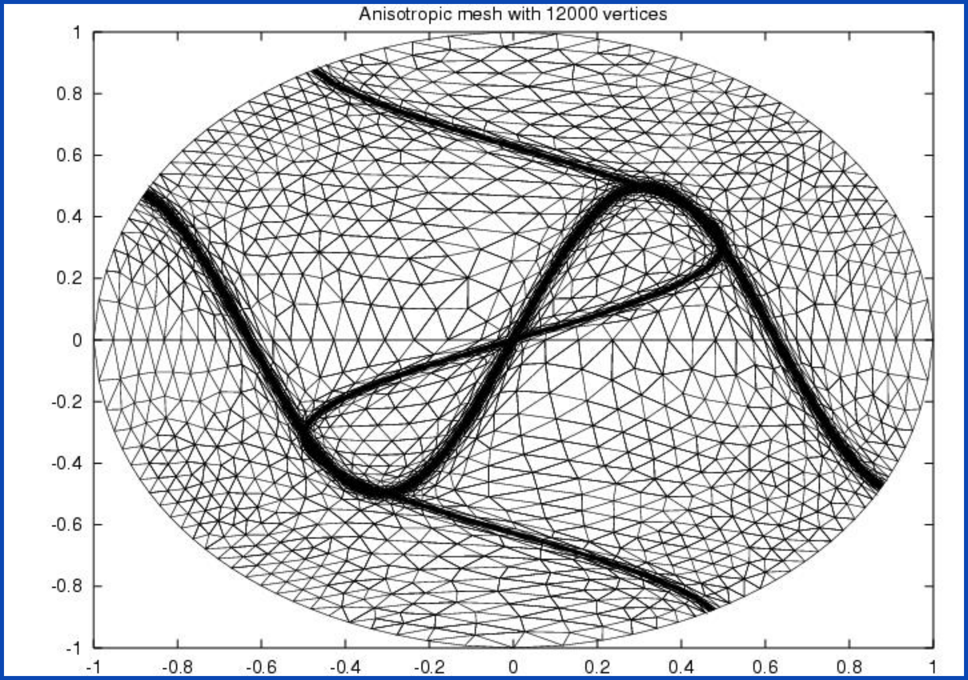

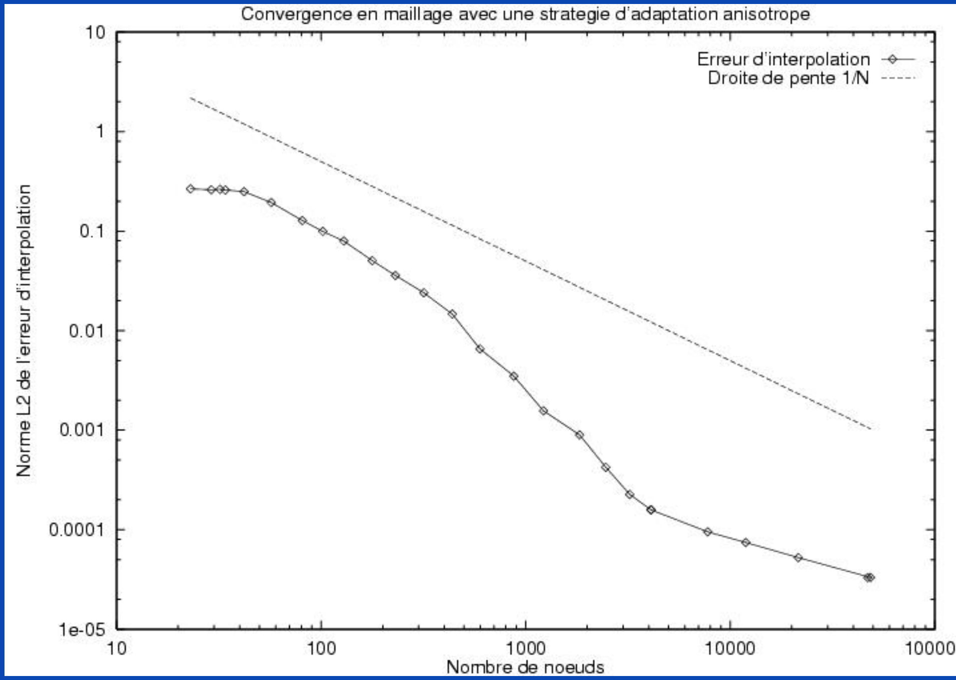

Lemma (barriers in L^2):

The convergence order of uniform refinement is at most 1/2,

The convergence order of 2D isotropic adaptative refinement is at most 1.

The convergence order of 3D isotropic adaptative uniform refinement is at most 3/4

Coudière-Dervieux-Leservoisier-Palmerio, 2001

N.B.: This was announced by the continuous metrics model, which produces "the best mesh". Analysis of the resulting error lead to the same barriers.

Illustration of the barrier lemma on a couple of two Heavyside functions

A vertical one and an horizontal one.

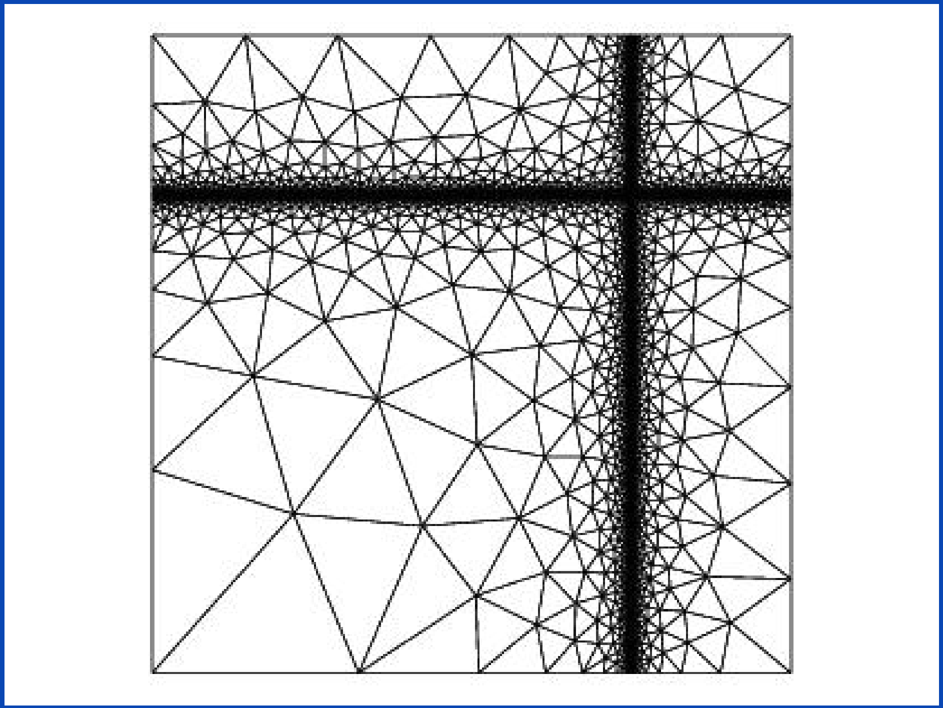

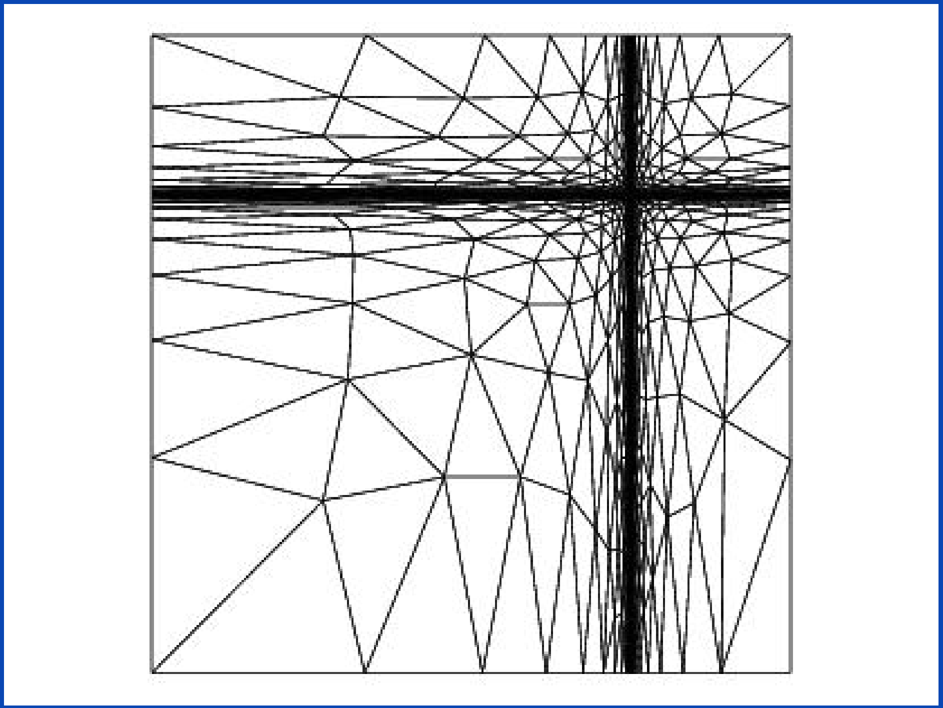

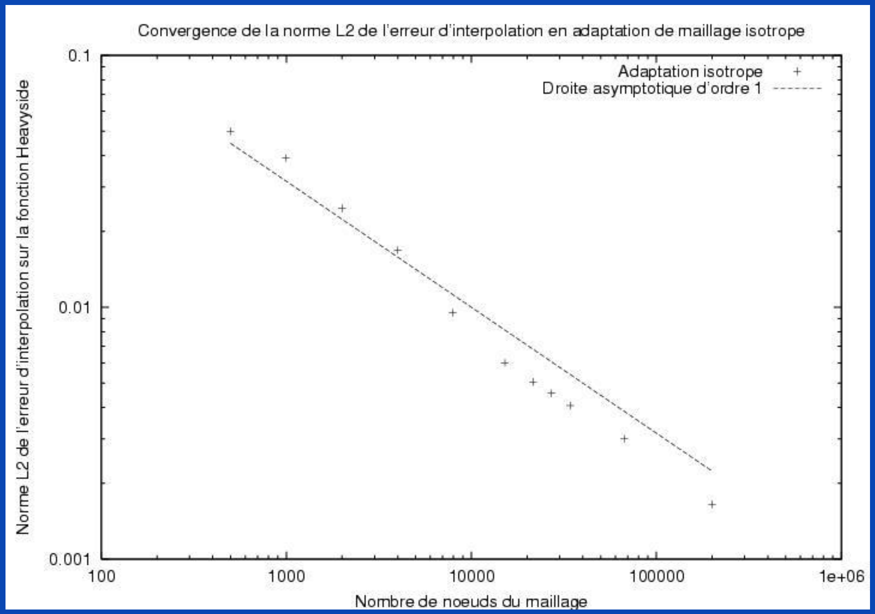

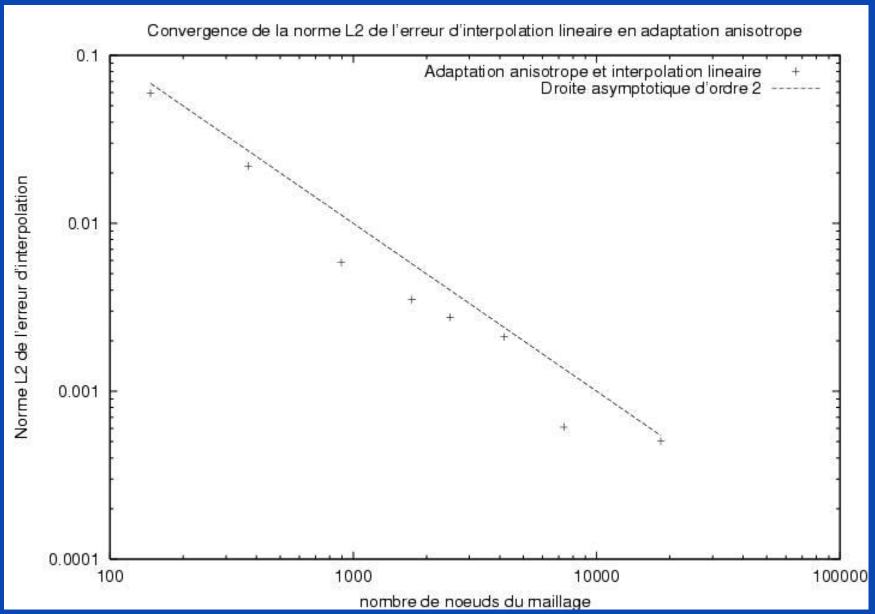

Isotropic : 1st order, anisotropic : 2nd order accuracy

BACK TO CONTINUOUS METRICS: EDP CASE

We return to the 1D continuous metrics method. $m(x)$ is local size of $h = \Delta x$.

$Au = f$ discretized by $A_h u_h = f_h$.

Error estimates:

$$u_h - u \quad = \quad A_h^{-1}(A_h u - f) \quad = \quad A^{-1}(A u_h - f)$$

The dependancy of u_h with respect to mesh size is not explicit and we shall prefer the first expression (*a priori estimate*).

CONTINUOUS METRICS FOR PDE : MODELLING

$$A_h u = Au + m^2 u_{xxx} = Au + m^2 D^3 u$$

$$f_h = f + m^2 f_{xx}$$

$$u_h - u = (A + m^2 D^3)^{-1} m^2 (|u_{xxx}| + |f_{xx}|)$$

For the sake of simplicity we prefer the main part of it:

$$u_h - u = A^{-1} m^2 (|u_{xxx|} + |f_{xx}|)$$

MINIMIZATION PROBLEM

In terms of $d = 1/m$:

$$\min \quad ||(Y(d)^2||^2_{L^2}$$

with constraint: $\int d(x)dx = N$.

State equation:

$$AY(d) \quad = \quad d^{-2}(h(u))$$

where $h(u) = |u_{xxx} - f_{xx}|$.

The (KKT) system to solve is :

$$\left\{ \begin{array}{l} A\,Y(d) \;=\; d^{-2}\,h(u) \qquad (State \;\; Equation) \\ \displaystyle\int d \;=\; N \\ A^{*}\Pi \;=\; Y \qquad (Adjoint \;\; equation) \\ < j'(d)\;,\,\delta d > \;=\; -\,2 < \Pi(d)\;,\,d^{-3}\,h(u)\;\delta d > \;=\; 0 \;\; \forall d, \displaystyle\int \delta d \;=\; 0 \end{array} \right. \tag{11}$$

We deduce from $\displaystyle\int \delta d \;=\; 0$ that

$$(\Pi(d))d^{-3}\;h(u) = constant$$

and thus ($h(u)$,Y,$\Pi > 0$),

$$d \;=\; Constant.((\Pi(d))^{T}\;h(u))^{1/3}$$

But $\int d = N$, then:

$$d = \frac{N}{\int ((\Pi(d))\ h(u))^{1/3}} . ((\Pi(d))\ h(u))^{1/3}$$

Then we can rewrite the (KKT) system as

$$\left\{ \begin{array}{l} A\ \bar{Y}(d) = \bar{d}^{-2}\ h(u) \qquad (State \quad Equation) \\ A^{*}\bar{\Pi} = \bar{Y} \quad (Adjoint \quad equation) \\ \bar{d} = \dfrac{1}{\int ((\bar{\Pi}(d))\ h(u))^{1/3}} . ((\bar{\Pi}(d))\ h(u))^{1/3} \end{array} \right. \qquad (12)$$

with $\bar{d} = \frac{d}{N}$, $\bar{Y} = N^2 Y$, $\bar{\Pi} = N^2 \Pi$.

Second order accuracy

$$j_{opt} \;=\; N^{-2}\int |\bar{Y}_{opt}|^2 \tag{13}$$

For "regular" discontinuities, $h(u) \in L^{\frac{1}{2}}$, we seek d in $L^{3/2}$.
Π is L^∞ and y is L^q, $\forall q < \infty$, then

$$\int |\bar{Y}_{opt}|^2 < \infty \tag{14}$$

which expresses *second order accuracy*.

CONVERGENCE CERTIFICATION

We return to the introductive airfoil example, a laminar flow with Mach=.85, and Reynolds= 73.
The sensor is the Mach number.

Second order convergence could not be obtained with a *uniformly refined* sequence of meshes with 3114, 12284, 48792 nodes.

The same convergence order measure is now applied to a sequence of *anisotropic adaptive* meshes with again 800, 3114, 12284, 48792 nodes.

CONVERGENCE CERTIFICATION : coarser meshes

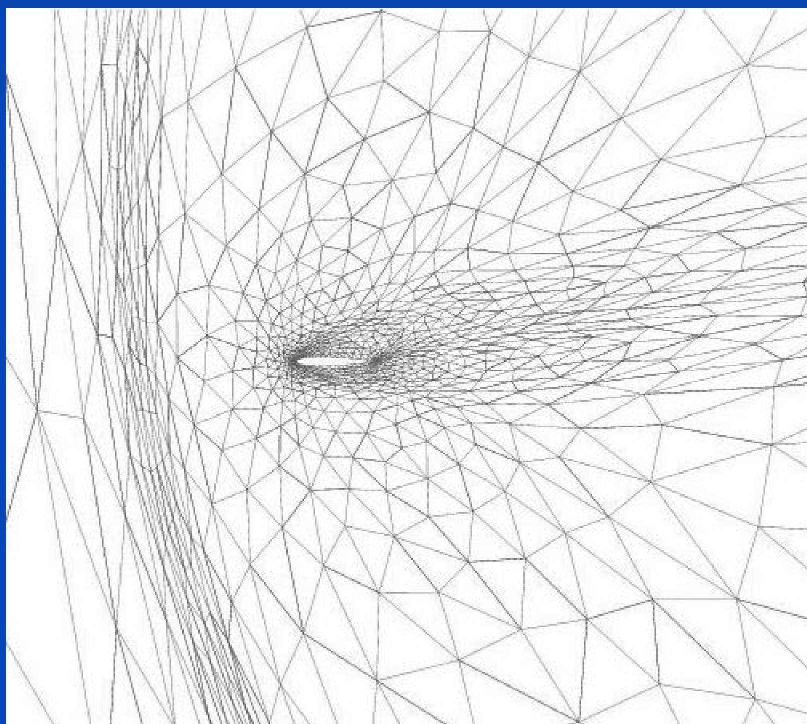

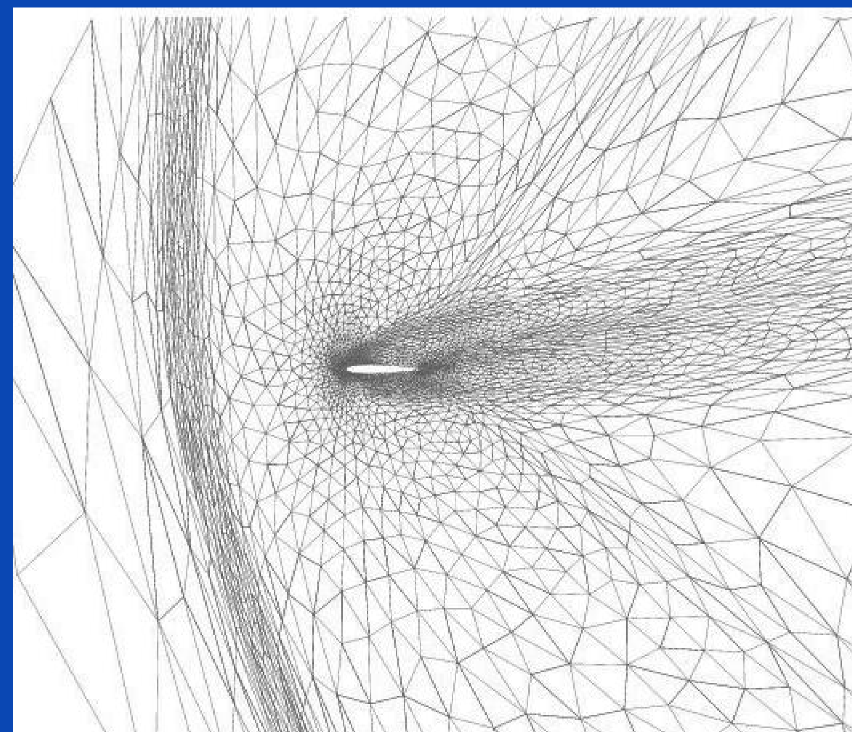

CONVERGENCE CERTIFICATION : finer meshes

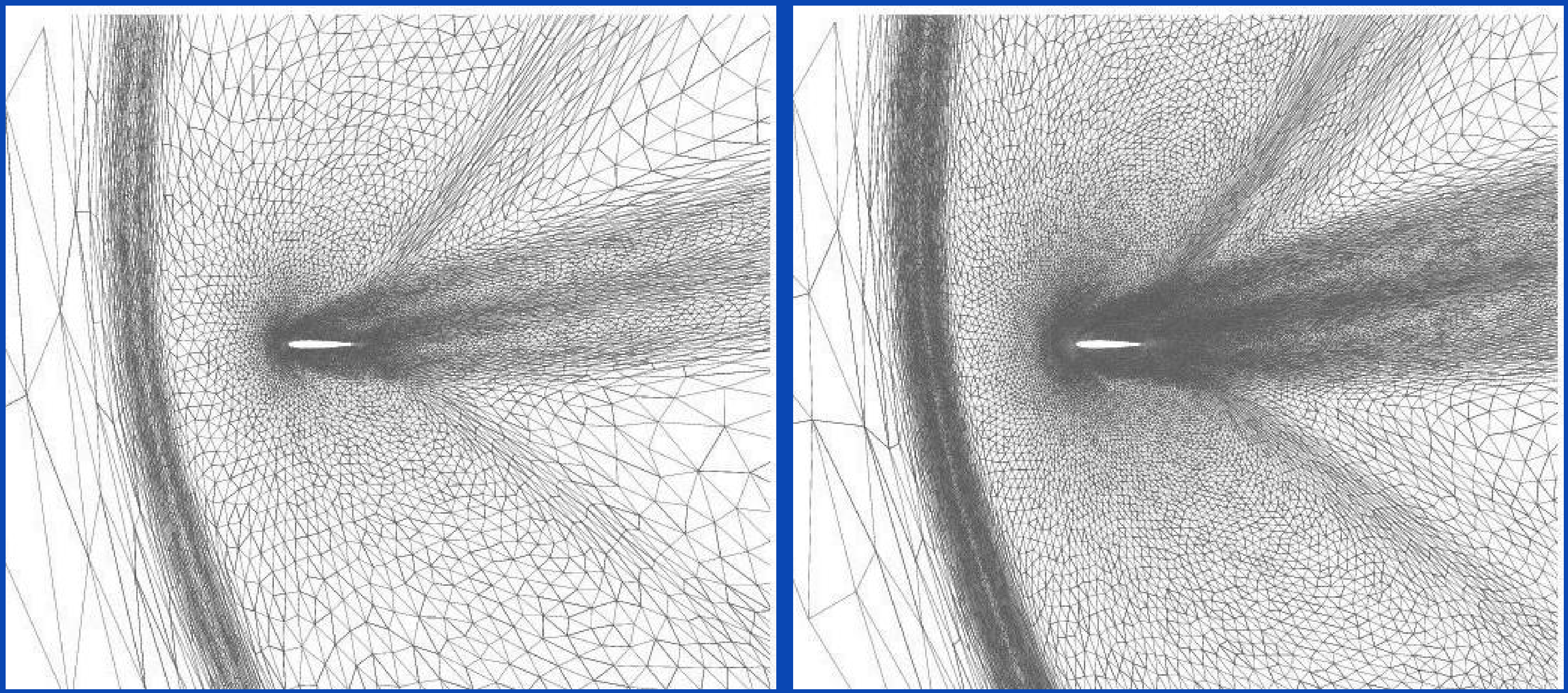

CONVERGENCE CERTIFICATION : convergence order

Certification of the convergence order in L^2:

Meshes 800, 3114, 12284 : convergence order for ρ,ρu,ρv : 1.75 (vs uniform refinement case : 0.94).

Meshes 3114, 12284, 48792 : convergence order for ρ,ρu,ρv : 1.92 (vs uniform refinement case : 1.14).

CONVERGENCE CERTIFICATION : Estimation of the global L^2 error

Meshes 800 (U_1), 3114 (U_2), 12284 (U_3) :

$$||U_3 - u||_{L^2} \ \leq \ \frac{1}{3}||U_2 - U_3||_{L^2} \ = \ 6.00 \ 10^{-5} \ .$$

Comparison with the 48792 mesh (U_4):

$$||U_3 - U_4||_{L^2} \ = \ 5.637 \ 10^{-5} \ .$$

I. MULTILEVEL PRECONDITIONING

1. Functional preconditioning:

$Min \quad \frac{1}{2}a(u,u) - (f,u)$, or, equivalently

$$A\,u \;=\; \Sigma\,(a_{ij}u_{x_j})_{x_i} \;=\; f \;\; on\;\Omega \;+\; Boundary\;Conditions$$

$$A_h\,u_h \;=\; f_h \;\; on\;\Omega$$

$$u_h^{n+1} \;=\; u_h^n \;-\; \rho(A_h\,u_h^n \;-\; f_h)$$

$$u^{n+1} \;=\; u^n \;-\; \rho \;\; B \;\; (A\,u^n \;-\; f)$$

Functional preconditioning, end'd

$$u_h^{n+1} \; = \; u_h^n \; - \; \rho^n \; B_h \; (A_h \; u_h^n \; - \; f_h)$$

- In case where $B = Id$, BA is **unbounded**, the first eigenmodes correspond to a *large number of high frequencies*. Convergence is mesh dependent and slowly improving with iterations.

- In case where BA is **continuous**, conditioning is best.

- In case where BA is **compact**, the first eigenmodes correspond to the *not so many low frequencies*.

In both latter cases mesh dependant convergence is possible.

2. Additive multilevel preconditioners (Bramble-Pasciak-Xu)

$(Au,v) = (f,v) \quad \forall u,v \in V_k$, f given in V'.

Let $(V_k)_{1\leq k\leq n}$ be a **hierarchy of subspaces** of V :

$V_1 \subset \cdots \subset V_k \subset \cdots \subset V_n \subset V$

For all $u \in V,\ \ v \in V_k$

$(Q_k u,v) = (u,v)$ "projector"

$(A_k u,v) = A(u,v) \forall u,v \in V_k$; λ_k spec. radius of A_k

$B_{BPX} \ = \ A_1^{-1} Q_1 \ + \ \sum_{k=2}^{n} \lambda_k^{-1}(Q_k - Q_{k-1})$

$B_{wavelets} \ = \sum_{k=1}^{n} \mu_k^{-1}(Q_k - Q_{k-1})$

3. Functional Standpoint:

$k = 1,\infty$.

the **functional preconditioner** :

$$B_{func} = \sum_{k=1}^{\infty} 2^{-(a+\alpha)}(Q_k - Q_{k-1}),$$

where Q_k is the **projector** on V_k and $\alpha > 0$,
is a **compact injection** :

$$H^s(\Omega) \rightarrow H^{s+a}(\Omega)$$

Kunoth 97, Courty 03

4. Extension to unstructured meshes : agglomeration

A. Agglomeration Coarsening

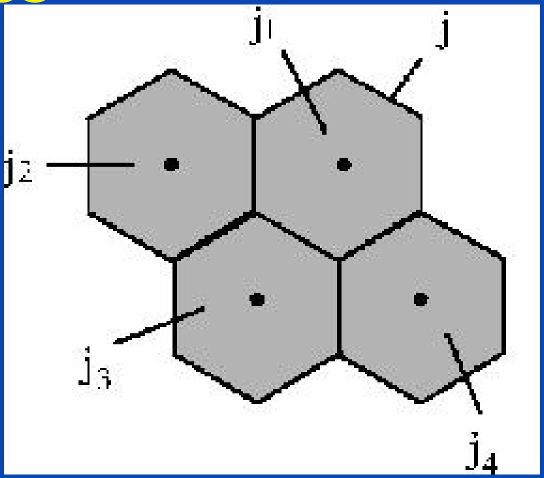

$$\Phi_I^{unsmooth}(i) \quad = \quad 1 \quad \text{if} \quad i \in S(I), \quad 0 \quad \text{otherwise.}$$

B. Smoothness

$$\Phi_I^{smooth} \; = \; \mathcal{L} \;\; \Phi_I^{unsmooth} \; ; \; V_k \; = \; Span[\Phi_1^{smooth}, \Phi_2^{smooth}, \ldots]$$

Marco-Dervieux, 95', Marco-Koobus-Dervieux 95'

APPLICATION TO SONIC BOOM REDUCTION

γ : control variable, the shape of the aircraft,
"CAD-free" parameterised by slipping of any skin vertex (along the fixed normal to initial shape (20,000 unknowns).

State(γ,W) : Steady 3D Euler eqs ($5\times$ 170,000 variables).
accounting for the shape through **transpiration conditions**.

$j(\gamma) = J(\gamma,W(\gamma))$ cost functional, a linear combination between :
- square deviation to target lift,
- square deviation to target drag,
- sonic boom emission model.

APPLICATION TO SONIC BOOM REDUCTION

Functional analysis:

A Hadamard derivative can be formally computed:
(see Bardos-Pironneau 2002 for rigorous derivations for hyperbolics)

It is an unbounded operator from $C^{l+\alpha}(\Gamma)$ to $C^{l-1+\alpha}(\Gamma)$

where Γ is the boundary to modify.

Then, the loss of derivative is (at least) 1.

Effect of preconditioning

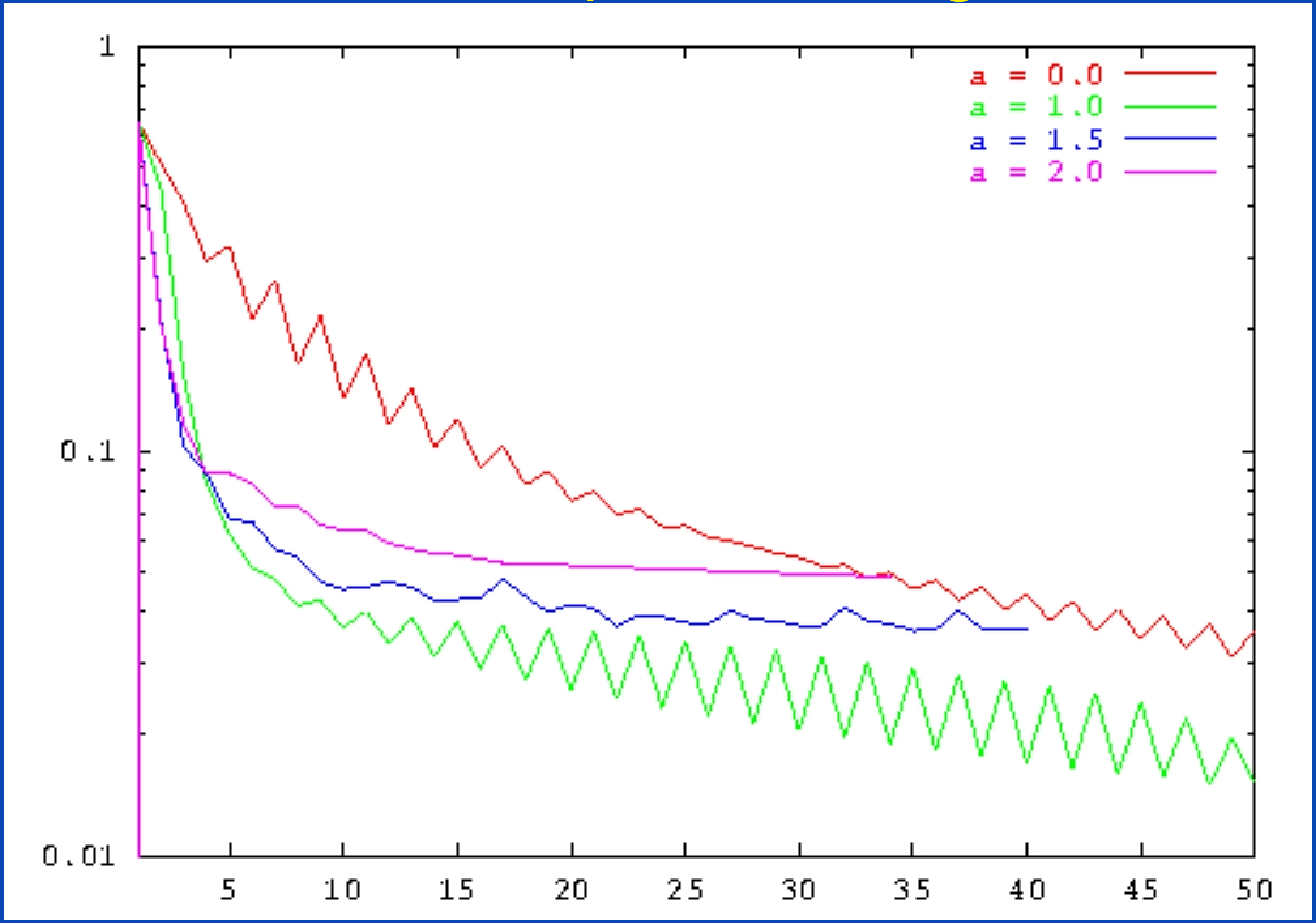

Optimisation of a wing with fixed drag and lift

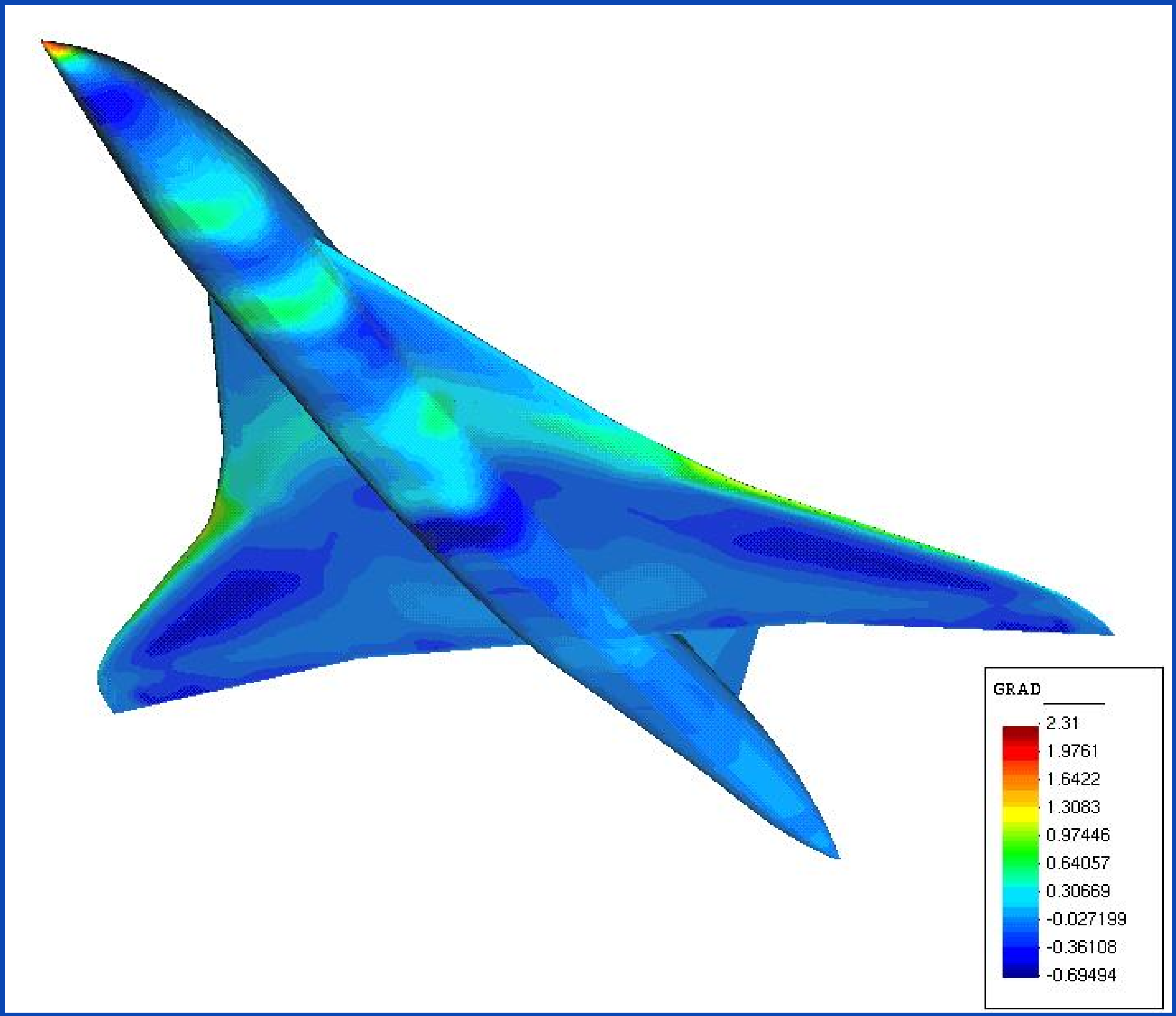

Optimisation of a wing with fixed drag and lift

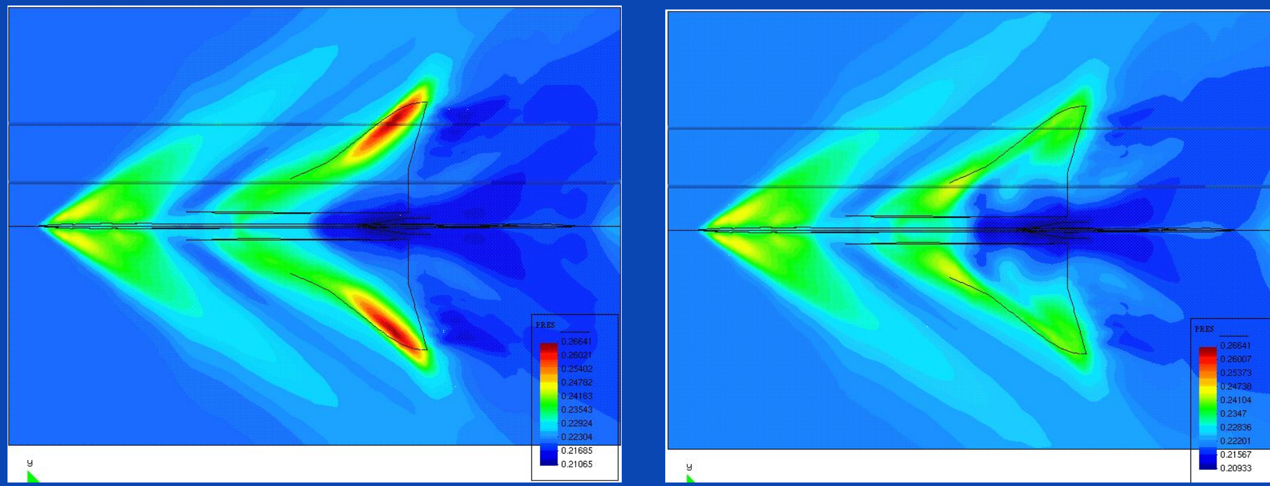

Pressure on a plan under the aircraft (10 itérations)

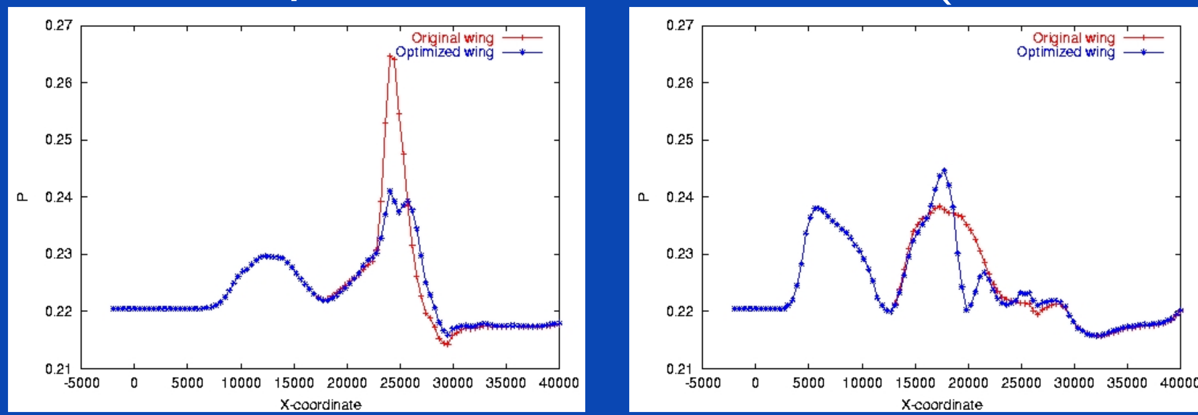

Two cut parallel to aircraft axis

CONCLUDING REMARKS

- **Steady case** Euler numerical prediction is rather well mastered and the global complexity for a prescribed error can be estimated:

$$O\left(\frac{1}{error}\log\left(\frac{1}{error}\right)\right).$$

- Solution of Shape Design optimality systems for steady models is also close to mastering.

- The unsteady computations on moving and/or adapted meshes set many open problems before an equivalent statement can be stated.

- This situation is even more severe with mixed numerical-physical models: LES, DES,...

NOTHING ON THIS PAGE

PDE's: THE ADAPTATION LOOP

Purpose : find mesh and *steady* solution with N nodes.

1.- build first mesh

2.- solve the PDE on the current mesh

3.- compute metrics from the PDE solution

4.- regenerate a mesh adapted to the metrics

5.- go to step 2 until iterative convergence

Iterative convergence : mesh and PDE solution do not change

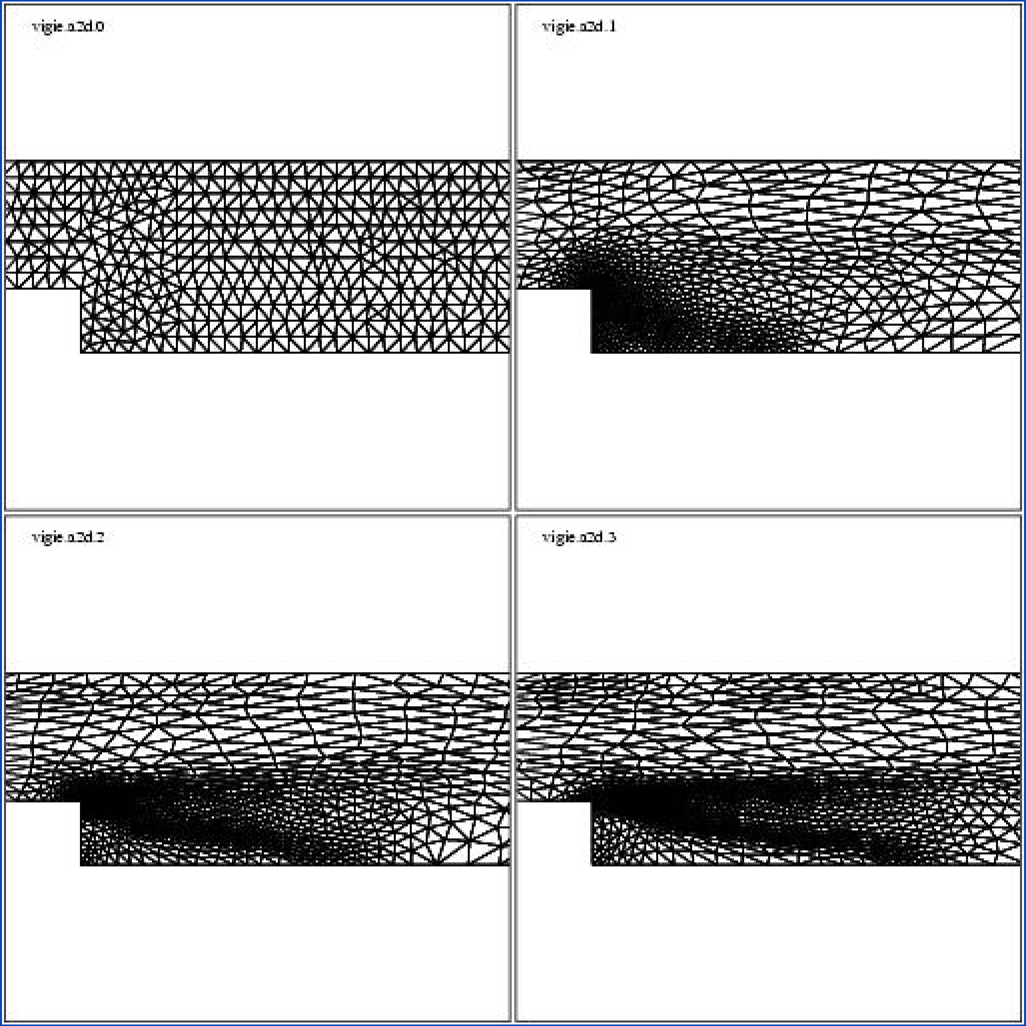

CONVERGENCE TO THE CONTINUOUS LIMIT:

We recommand this be a different loop from the adaptation loop.

Therefore “convergence to the limit” is an *external loop* to the adaptation loop.

- Vary N from small to large:

Standard choice: N, $4N$, $16N$.

PDE's : MAIN OPTIONS

- Steady Reynolds-Average Navier-Stokes equations for compressible flow, $k-\varepsilon$ model with wall laws. Wall law thickness is specified by user, not by the mesh.

- Same vertex centered upwind (Roe) second-order (Van Leer) approximation with P1-FEM for viscous terms.Implicit pseudo-unsteady solution algorithm.

- $A\ priori$ sensor (**):

$|u-u_h| \ \leq \ K\ (\delta x,\delta y)^t|H|(\delta x,\delta y)$ with H Hessian of Mach number.

- Experiment protocol: compare several medium-mesh calculations with a very accurate “reference” one.

(*) George-Hecht-Mohammadi, Fortin and coworkers

EXAMPLES : 1. Flat plate test case (supersonic)

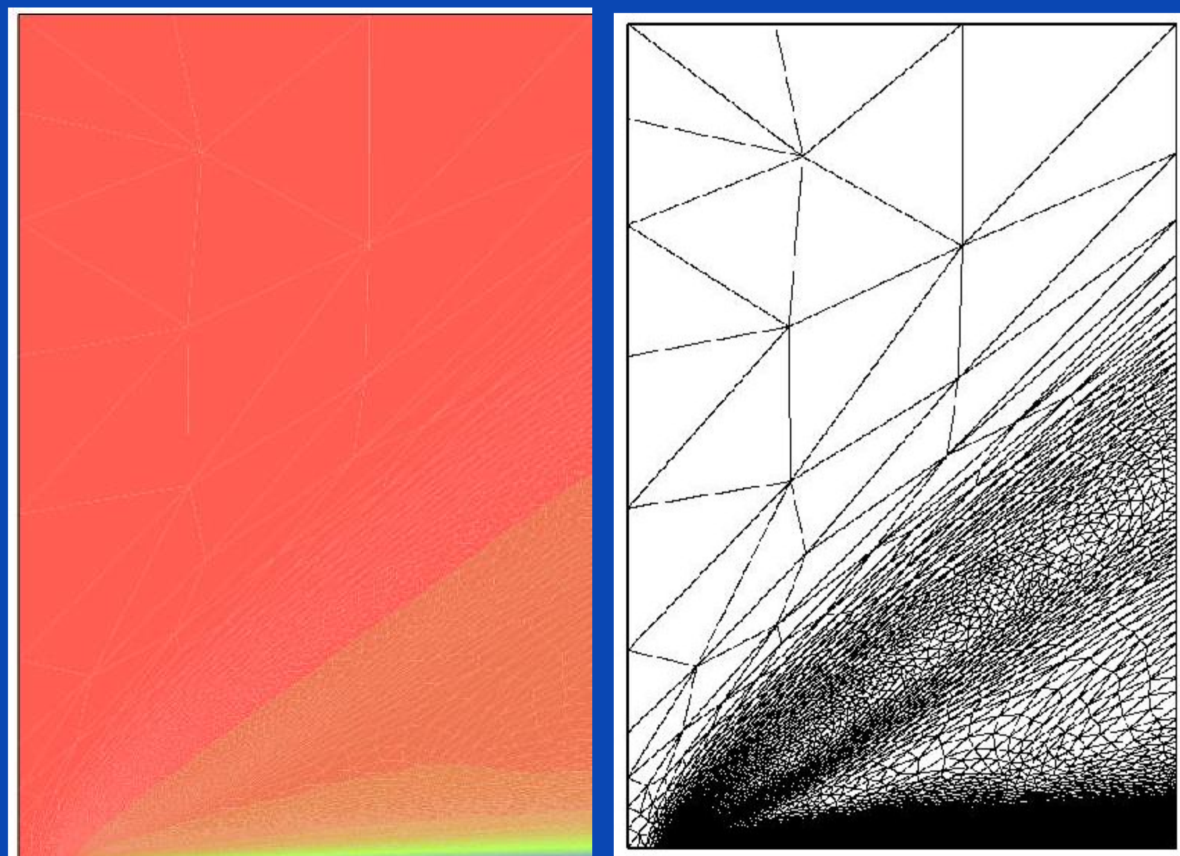

Reference fine mesh, 40,000 nodes and solution (Mach contours)

Flat plate test case : convergence

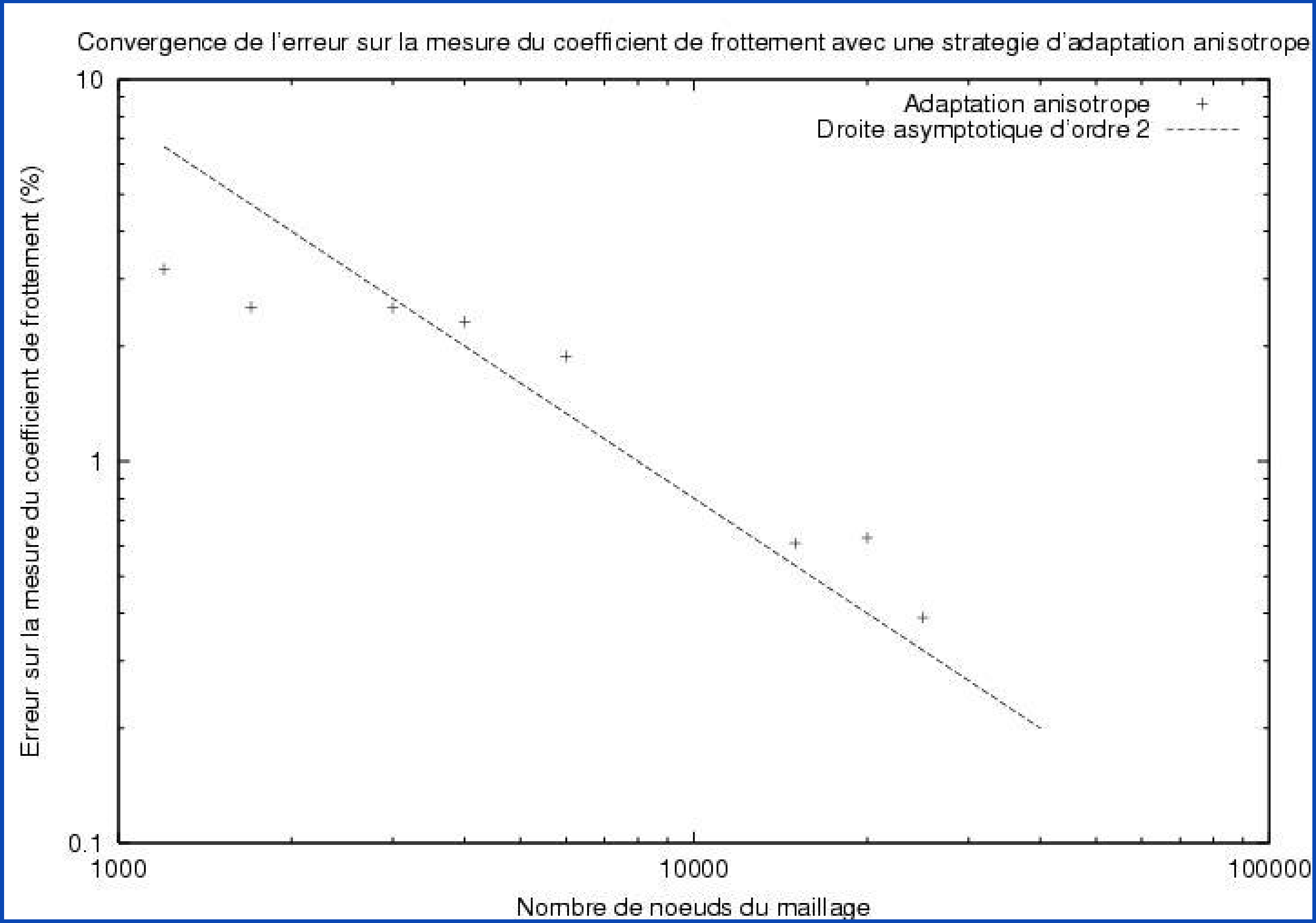

EXAMPLES : 2. Back step flow (slightly compressible)

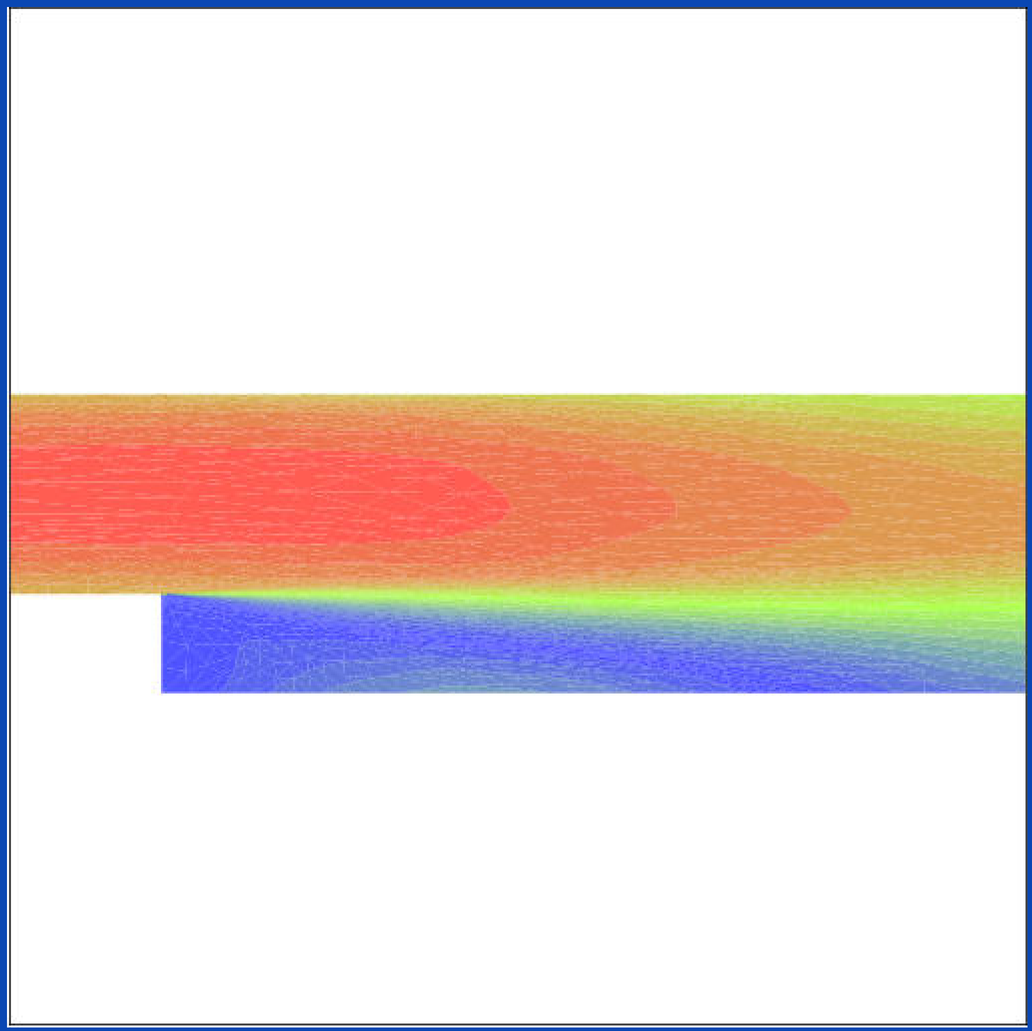

EXAMPLES : 2. Back step flow (slightly compressible)

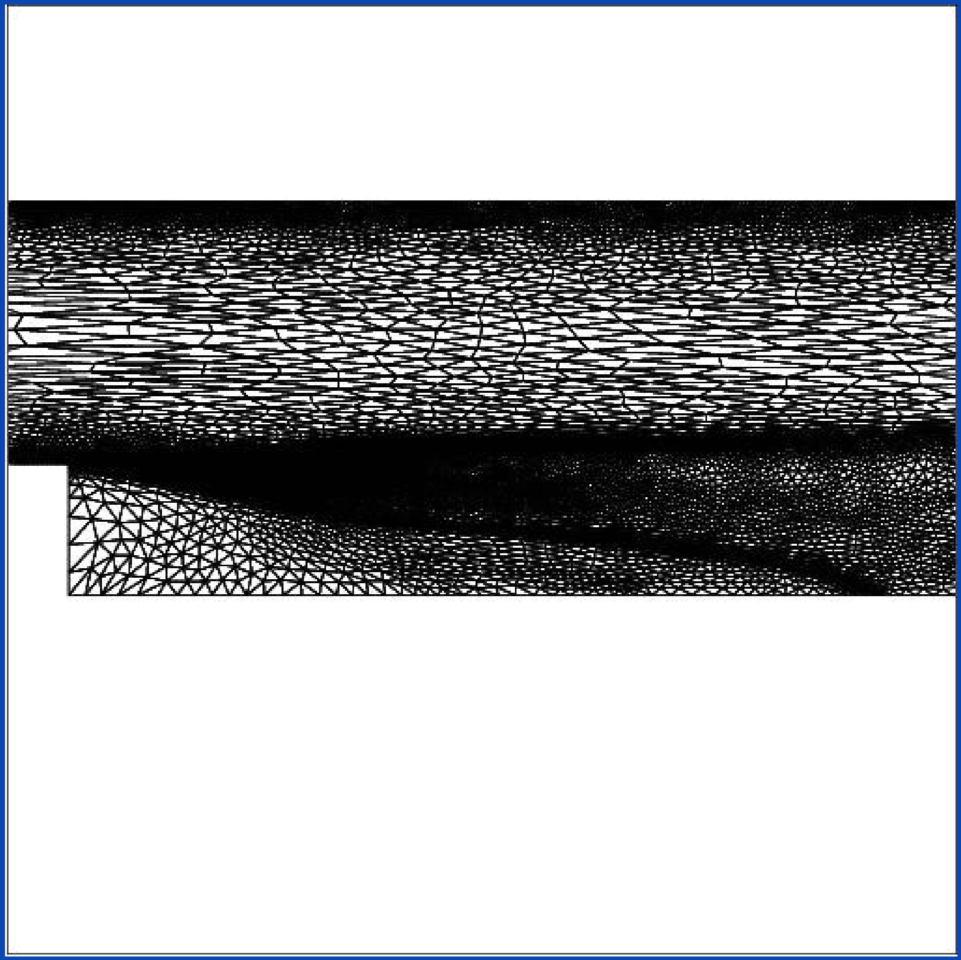

Reference mesh, 25 Knodes (large Y^+, reattachment abscissa:

$6.6H$)..

EXAMPLES : 2. Back step flow (slightly compressible)

Convergence of reattachment abscissa.